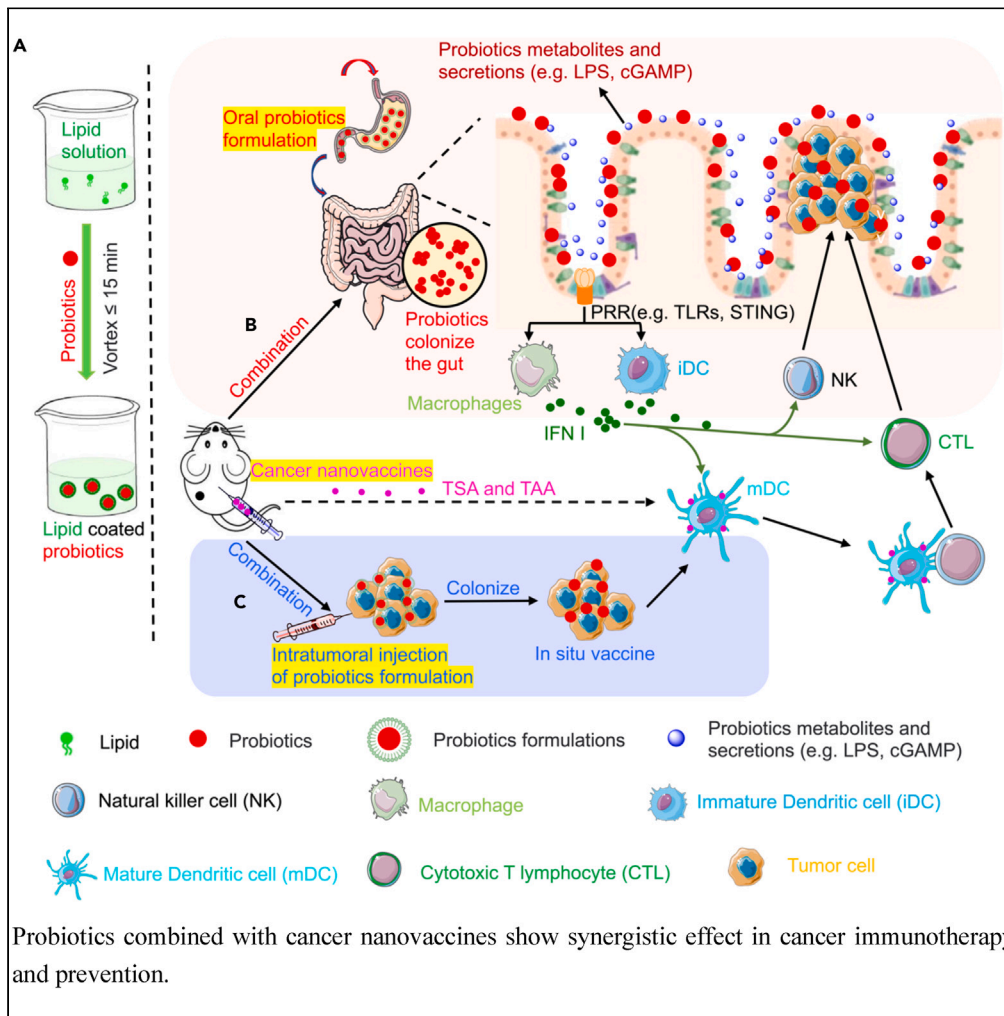


Article

# Probiotics formulation and cancer nanovaccines show synergistic effect in immunotherapy and prevention of colon cancer



Xiangxiang Xu,  
Meng Zhang,  
Xiaoyan Liu, ...,  
Yipeng Wang,  
Fengfeng Mo, Mi  
Liu

mofengfeng@smmu.edu.cn  
(F.M.)  
mi.liu@suda.edu.cn (M.L.)

**Highlights**  
Probiotics coated with  
lipid membrane can  
facilitate the cancer  
therapy and prevention

Proper probiotics  
formulation combine with  
cancer vaccine can  
prevent and treat cancer

The probiotics facilitated  
the induction of tumor  
antigen-specific cytotoxic  
T cells

Probiotics formulation can  
alter the  
microenvironment in  
colon

Xu et al., iScience 26, 107167  
July 21, 2023 © 2023 The  
Author(s).  
[https://doi.org/10.1016/  
j.isci.2023.107167](https://doi.org/10.1016/j.isci.2023.107167)



## Article

## Probiotics formulation and cancer nanovaccines show synergistic effect in immunotherapy and prevention of colon cancer

Xiangxiang Xu,<sup>1,2,3,5</sup> Meng Zhang,<sup>1,5</sup> Xiaoyan Liu,<sup>1</sup> Mingze Chai,<sup>1</sup> Lu Diao,<sup>1,2,3</sup> Lin Ma,<sup>2</sup> Shuang Nie,<sup>4</sup> Minghao Xu,<sup>1,3</sup> Yipeng Wang,<sup>1</sup> Fengfeng Mo,<sup>4,\*</sup> and Mi Liu<sup>1,2,3,6,\*</sup>

## SUMMARY

**Probiotics play essential roles in immune modulation. Combining probiotics with cancer vaccines potentially can achieve a synergistic effect. To maximize the efficacy of probiotics, proper probiotics formulation is necessary. Herein, *Lactobacillus rhamnosus* and *Bifidobacterium longum* are coated with lipid membrane to achieve the goal of losing less activity and bettering colonization in colon. In the subcutaneous transplanted colon cancer mouse model, probiotics formulation showed potent preventive and therapeutic efficacy, and the efficacy could be further improved by combining with cancer nanovaccines. Probiotics formulation can perform as immune adjuvants to enhance the innate immune response or as *in-situ* cancer vaccines. In the study of preventing chemical-induced orthotopic colon cancer model, probiotics formulation alone efficiently reduced tumor number in colon and the efficacy is improved by combining with cancer nanovaccines. All in all, the studies demonstrated that probiotics formulation can assist to maximize the efficacy of cancer nanovaccines.**

## INTRODUCTION

Colon cancer is one of the most aggressive cancers in the world,<sup>1</sup> accounting for 11% of all newly diagnosed malignant diseases worldwide,<sup>2,3</sup> and approximately 20% of colon cancer patients have metastasis when diagnosed.<sup>4</sup> Surgical resection is the main treatment for early stage of colon cancer, and adjuvant therapy can improve the chance of cure in high-risk patients.<sup>5</sup> To prevent complications such as intestinal obstruction, intestinal perforation, or bleeding, removal of primary tumors followed by systemic chemotherapy is necessary to treat metastasis, but the efficacy and biosafety need to be further improved at present.<sup>6</sup>

The complex microbial community in colon is essential to maintain homeostasis, regulate metabolic functions, support the intestinal barrier, and control the immune responses. Therefore, changes in the composition and diversity of microbes in the intestine are considered to be critical to the generation, proliferation and progression of tumors.<sup>7–9</sup> At the same time, previous studies have supported the existence of crosslink between the gut microbiota and colorectal cancer, so the management of gut microbiota may become a strategy to suppress the occurrence and progression of colon cancer.<sup>10–12</sup>

Currently, the gut microbiome has been identified as an important regulator of cancer progression and treatment, studies have shown that the local microbiome is an important component in the tumor micro-environment in many types of cancers, especially in colon cancer. Growing evidence suggests that gut microbiota, especially probiotics, can be used to enhance the antitumor efficacy of cancer immunotherapy, small molecules released by probiotics such as LPS and cGAMP can act on intestinal pattern recognition receptors and activate the innate immune system, promote the secretion of type I interferons, effectively recruit and accelerate the maturation of dendritic cells, activate T cells and NK cells, which acts as an immune adjuvant to affect the occurrence and development of cancer.<sup>13,14</sup>

Cancer vaccines, especially cancer nanovaccines reassembled from whole components of tumor cells, can activate tumor antigen-specific T cells, which is the main killer of cancer cells, and thus control tumor growth. It is a process needs days or even weeks to efficiently activate such tumor antigen-specific

<sup>1</sup>College of Pharmaceutical Sciences, Soochow University, Suzhou, Jiangsu 215123, People's Republic of China

<sup>2</sup>Kunshan Hospital of Traditional Chinese Medicine, Kunshan, Jiangsu 215300, People's Republic of China

<sup>3</sup>Suzhou Ersheng Biopharmaceutical Co., Ltd, Suzhou 215123, People's Republic of China

<sup>4</sup>Department of Nutrition and Food Hygiene, Faculty of Naval Medicine, Naval Medical University, 800 Xiangyin Rd, Shanghai 200433, People's Republic of China

<sup>5</sup>These author contributed equally

<sup>6</sup>Lead contact

\*Correspondence: mofengfeng@smmu.edu.cn (F.M.), mi.liu@suda.edu.cn (M.L.)  
<https://doi.org/10.1016/j.isci.2023.107167>



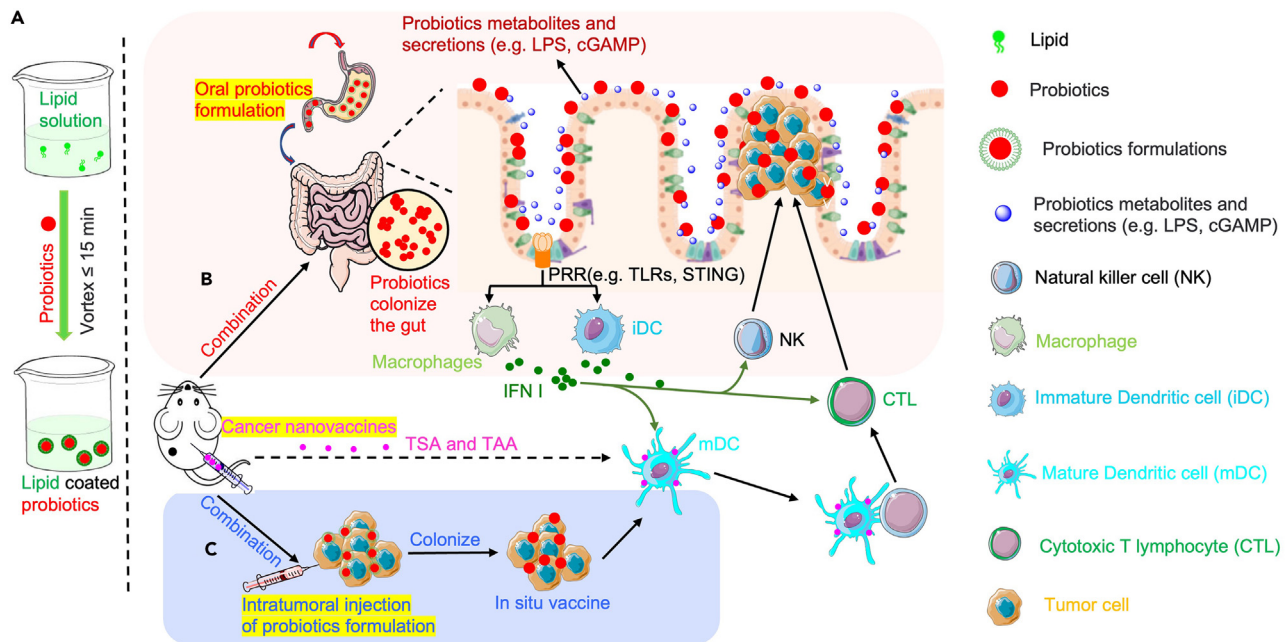


**Figure 1. Schematic illustration of combined application of probiotics formulation and cancer vaccines**

(A) Preparation of probiotics formulation.

(B) Schematic diagram of probiotics formulation orally administration combined with nanovaccines.

(C) Schematic diagram of probiotics formulation intratumoral administration combined with nanovaccines.

T cells by cancer vaccines, and thus substances such as probiotics may intervene the T cell activation process and promote the activation of antigen-specific T cells.

Studies have reported *Lactobacillus rhamnosus* (LGG) and *Bifidobacterium longum*'s functions in anti-inflammatory, anti-cancer, anti-metastasis,<sup>15–18</sup> and enhancing the function of dendritic cells, and specifically augmenting T cell responses.<sup>19,20</sup> In addition, *B. longum* administration could reduce intestinal inflammation without impairing the antitumor function of CTLA-4 in mice.<sup>21</sup>

Though applying LGG and *B. longum* as a cancer immunotherapy method seems promising, directly application especially orally administration, for cancer treatment faces various challenges. These including: (1) biochemical barrier, such as acidic gastric juice, which can inactivate probiotics;<sup>22</sup> (2) physical barrier, such as rapid gastrointestinal peristalsis limits the retention and colonization of probiotics in the intestine.<sup>23</sup> Therefore, it is necessary to formulate probiotics to evade these obstacles and achieve better immune efficacy. One strategy is using molecular materials such as alginate,<sup>23,24</sup> chitosan,<sup>23</sup> polydopamine,<sup>25</sup> lipids,<sup>26,27</sup> etc.<sup>28</sup> to synthesize microbial surface coatings to enhance the resistance of microorganisms against adverse environments. However, the preparing method and the materials used may lead to the decrease of the activity of bacteria and thus affect the therapeutic effect. Hence, enhancing probiotics delivery efficiency without compromising safety is a central challenge in microbial therapy for cancer.<sup>29</sup>

Herein, we reported an approach enabled self-assembled biofilm to encapsulate bacteria to optimize the efficacy of probiotics and avoid loss of activity. Such formulation could improve the ability of probiotics to against the complex environment of the gastrointestinal tract,<sup>30</sup> to enhance the innate immune response when orally administered, and colonize sufficiently in tumor microenvironment as *in-situ* cancer vaccines.<sup>31</sup> Thus probiotics formulation can display synergetic immune effects when combined with cancer nanovaccines reassembled from whole components of tumor tissues, which showed potent preventive and therapeutic efficacy in various cancers.<sup>32,33</sup> The combination treatment can activate innate and adaptive immune responses through multiple ways, and probiotics can activate innate immunity and intervene in the T cell activation process to help cancer nanovaccine to activate antigen-specific T cells more efficiently (Figure 1). Besides, this combined treatment mode has obvious advantages in terms of biological safety compared to the combined methods currently used in clinical practice.

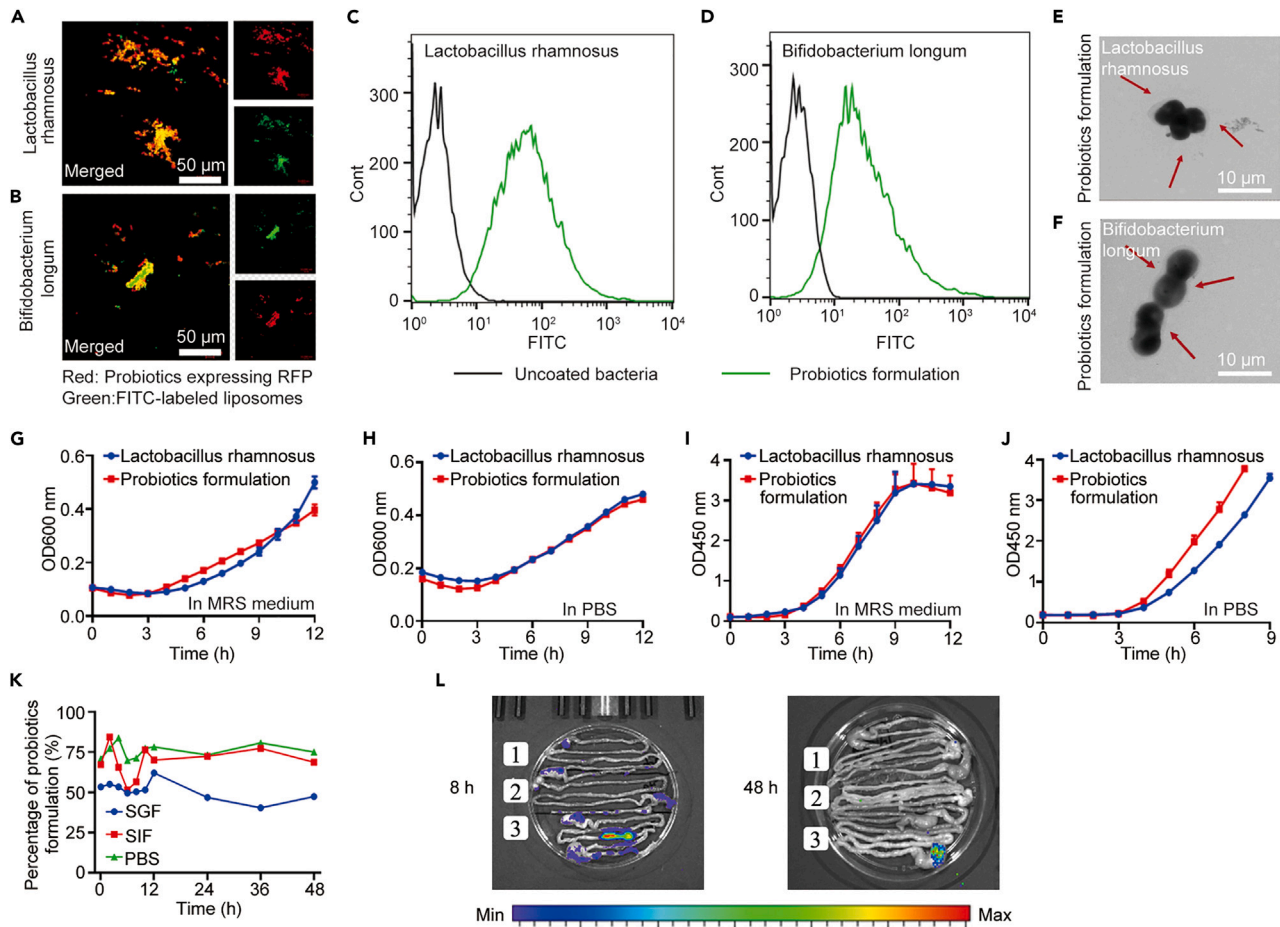


**Figure 2. Characterization of probiotics formulations and activity test of probiotics formulation and GI track retention test. Representative LSCM images of *Lactobacillus rhamnosus***

(A) and *Bifidobacterium longum* (B) based probiotics formulation (scale bar: 50  $\mu\text{m}$ , Red: Probiotics expressing RFP, Green: FITC-labeled liposomes, Yellow: Merged). Flow cytometric analysis of FITC-labeled probiotics formulation (*Lactobacillus rhamnosus* (C) and *Bifidobacterium longum* (D)). Representative TEM images of *Lactobacillus rhamnosus* (E) and *Bifidobacterium longum* (F) based probiotics formulation (scale bar: 10  $\mu\text{m}$ ).

(G and H) The growth curves of LGG/probiotics formulation in MRS medium/PBS.

(I and J) The cell viability of LGG/probiotics formulation in MRS medium/PBS.

(K) Flow cytometric analysis of probiotics formulation after incubation in SGF/SIF/PBS.

(L) Representative IVIS images of mouse intestinal tracts after oral gavage of PBS (1), naked *Escherichia coli* carrying pGEN- luxCDABE (2) and LCB (3) for 8 h/48 h.

## RESULTS

### Probiotics formulation preparation and characterization

To prepare lipid membrane-coated probiotics, a lipid solution was first made, and then vortexed with the bacterial solution for at most 15 min to obtain the final products (Figure 1A). Among them, the lipid membrane was labeled with FITC (green fluorescence), and the bacteria themselves could express RFP (red fluorescence), so that it was convenient to confirm whether the lipid membrane was successfully coated. Figures 2A and 2B were representative colocalization images of the red fluorescent bacteria and the lipid membrane labeled with FITC green fluorescence. A yellow color overlap could be seen after fusion, indicated that the successfully coating of lipid membrane over probiotics. Flow cytometry was also applied to verify whether the lipid membrane was successfully coated or not. Compared with the naked probiotics, the fluorescence intensity of FITC was significantly increased in probiotics formulation (Figures 2C and 2D), indicating that the bacteria were successfully encapsulated by the lipid membrane. Figures 2E and 2F were electron microscope images of probiotics formulation, while the black part was the bacteria. After coating, the particle size and potential become larger, indicating that the lipid membrane was successfully coated (Figure S1).

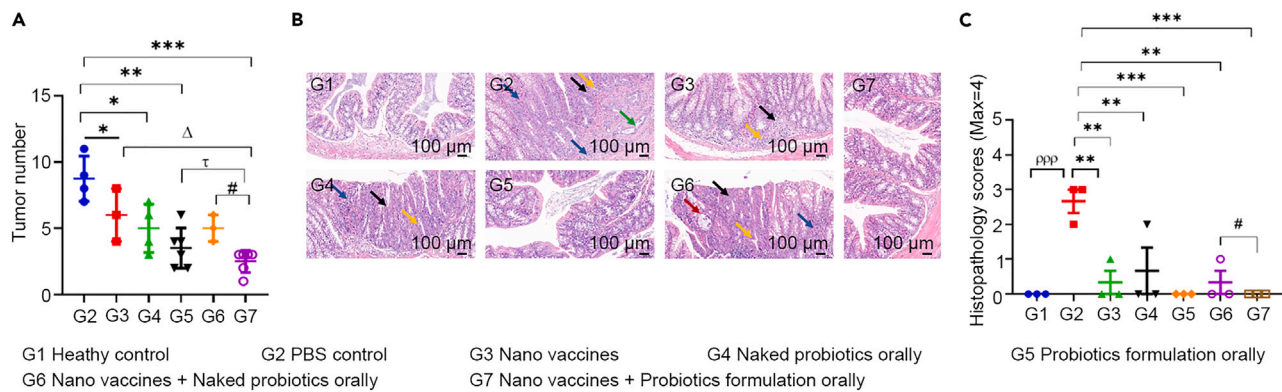


**Figure 3. Analysis of the efficacy of probiotic formulations (orally administration) and nanovaccines in preventing AOM/DSS-induced orthotopic colon cancer**

(A) The number of colon tumors in mice with various treatments.

(B) H&E staining analysis of mouse colon of each group (1000 $\times$ , scale bar: 100  $\mu$ m).

(C) The pathological scores of the colons in each group after H&E staining (n = 3). \*,  $\tau$ , # and  $\Delta$  means significant difference and  $p \leq 0.05$ ; \*\* means significant difference and  $p \leq 0.01$ ; \*\*\* and  $ppp$  means significant difference and  $p \leq 0.005$ .

### Growth and vitality analysis of probiotics formulation

To evaluate the influence of activity of bacteria after lipid film coating, we analyzed the growth of the bacteria in the probiotic formulation. After 12 h incubation, the growth status of probiotics formulation in MRS/PBS medium was similar to naked bacteria, indicating the rare influence of lipid film on bacteria's activity (Figures 2G–2J).

### In vitro resistance of probiotics formulation against GI tract environment

Subsequently, the retention time of probiotics formulation in the simulated gastric fluid and intestinal fluid was evaluated. It was found that the lipid film could protect the bacteria to survive for up to 48 h (Figure 2K).

### In vivo resistance of probiotics formulation against GI tract environment

To verify probiotics formulation's retention time in the gastrointestinal tract, the residual bacteria in the gastrointestinal tract of mice fed with  $1 \times 10^8$  CFU bacteria by gavage was tested at 8 h and 48 h (Figure 2L). After 48 h, the fluorescence intensity of probiotics formulation group was higher than that of the naked bacteria group, indicating that the lipid membrane could prolong the gastrointestinal retention time of bacteria.

### Probiotics effectively prevented the orthotopic colon cancer

In the prevention of AOM/DSS-induced orthotopic colon cancer, the administration schedule of each group of mice was shown in Figure S2. The results showed that, compared to the control group, both nanovaccines and probiotics reduced the number of colon tumors in the mice, and combining nanovaccines with probiotics formulation together further significantly decreased the number of tumors in treated mice (Figure 3). These results implied probiotics formulation's alone potential preventive effect on orthotopic colon cancer, and more satisfactory efficacy could further be achieved by combining with cancer nanovaccines.

### Analysis of microenvironment in colon in mouse orthotopic colon cancer model after treatment with probiotics formulation

Colons of AOM/DSS-induced orthotopic colon cancer bearing mice, undergoing orally administrating of probiotics and subcutaneously injecting of nanovaccines, were collected and investigated by H&E staining and pathological analysis. Healthy mice without any treatment were applied as healthy control (Figures 3, 4, and 5).

The healthy control group exhibited a clear structure of colonic folds, and an integrated structure of the mucosal intestinal epithelium, which was a single layer of columnar epithelium. The morphology and

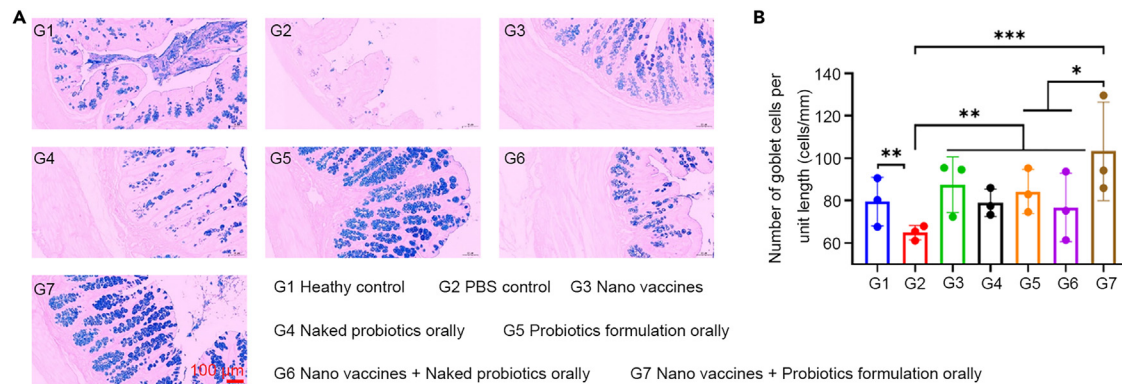


**Figure 4. Analysis of colonic goblet cells in mice in each group after AOM/DSS treatment induction of colon cancer**

(A) The AB/PAS staining analysis images of the colons of the mice in each group (200 $\times$ , scale bar: 100  $\mu$ m).

(B) The number of goblet cells per unit length of the colons of the mice in each group after AB/PAS staining (n = 3). \* Means significant difference and  $p \leq 0.05$ ; \*\* means significant difference and  $p \leq 0.01$ ; \*\*\* means significant difference and  $p \leq 0.005$ .

structure of epithelial cells were normal, and the number of intestinal glands and goblet cells were abundant in the lamina propria. The muscle layer was evenly stained, the muscle fibers were normal in structure and regular arrangement, no obvious inflammation was found.

In the PBS group, mucosal layer displayed epithelial cell hyperplasia (black arrow) and mitotic figures (yellow arrow), the number of goblet cells decreased, presented punctate necrosis of individual epithelial cells and nuclear fragmentation (red arrow), and lymphocyte spots infiltration (blue arrow) was also appeared.

In the mice treated with nanovaccines, epithelial cell proliferation (black arrow) was seen in the mucosal layer, the number of goblet cells was significantly reduced, accompanied by punctate infiltration of lymphocytes and neutrophils (blue arrows).

In the mice treated with naked bacteria, there was more epithelial cell proliferation (black arrows) in the mucosal layer, mitosis (yellow arrows) was suspected to be tumor cells, the number of goblet cells was reduced, and there was a small amount of lymphocytes infiltration (blue arrows).

In the mice treated with probiotics formulation, the structure of colonic folds was clear and integrated, the mucosal intestinal epithelium was consisted by a normal single-layer columnar epithelium. The morphological structure of epithelial cells was rarely affected, the number of intestinal glands in the lamina propria was abundant, and many goblet cells could be seen. The muscle layer was evenly stained, the muscle fibers exhibited normal structure and regular arrangement, and there was no obvious inflammation.

In the mice treated with nanovaccines plus naked probiotics, more epithelial cell proliferation (black arrow) presented in the colonic mucosal layer, mitosis (yellow arrow) was suspected to be tumor cells, and some proliferated epithelial cells were found to enter the submucosa (green arrow). The number of goblet cells was reduced with small number of lymphocytes infiltration (blue arrows).

In the mice treated with nanovaccines plus probiotics formulation, the structure of colonic folds and mucosal intestinal epithelium were clear and normal. The number of intestinal glands in the lamina propria and goblet cells were abundant. The muscle layer and muscle fibers were normal in structure and regular arrangement, with no obvious inflammation.

From the morphological presentation and pathological scores obtained from H&E staining, mice treated with nanovaccines plus probiotics formulation exhibited significantly reduced inflammation compared to PBS control group, indicating the synergetic preventive effect of probiotics formulation combined with cancer nanovaccines in AOM/DSS induced orthotopic colon cancer bearing mice (Figure 3).

Intestinal goblet cells (GCs) are differentiated from intestinal mucosal basal stem cells and contain mucus-containing granules, so they can secrete mucus into intestinal epithelial cells to form a mucus layer to fill the

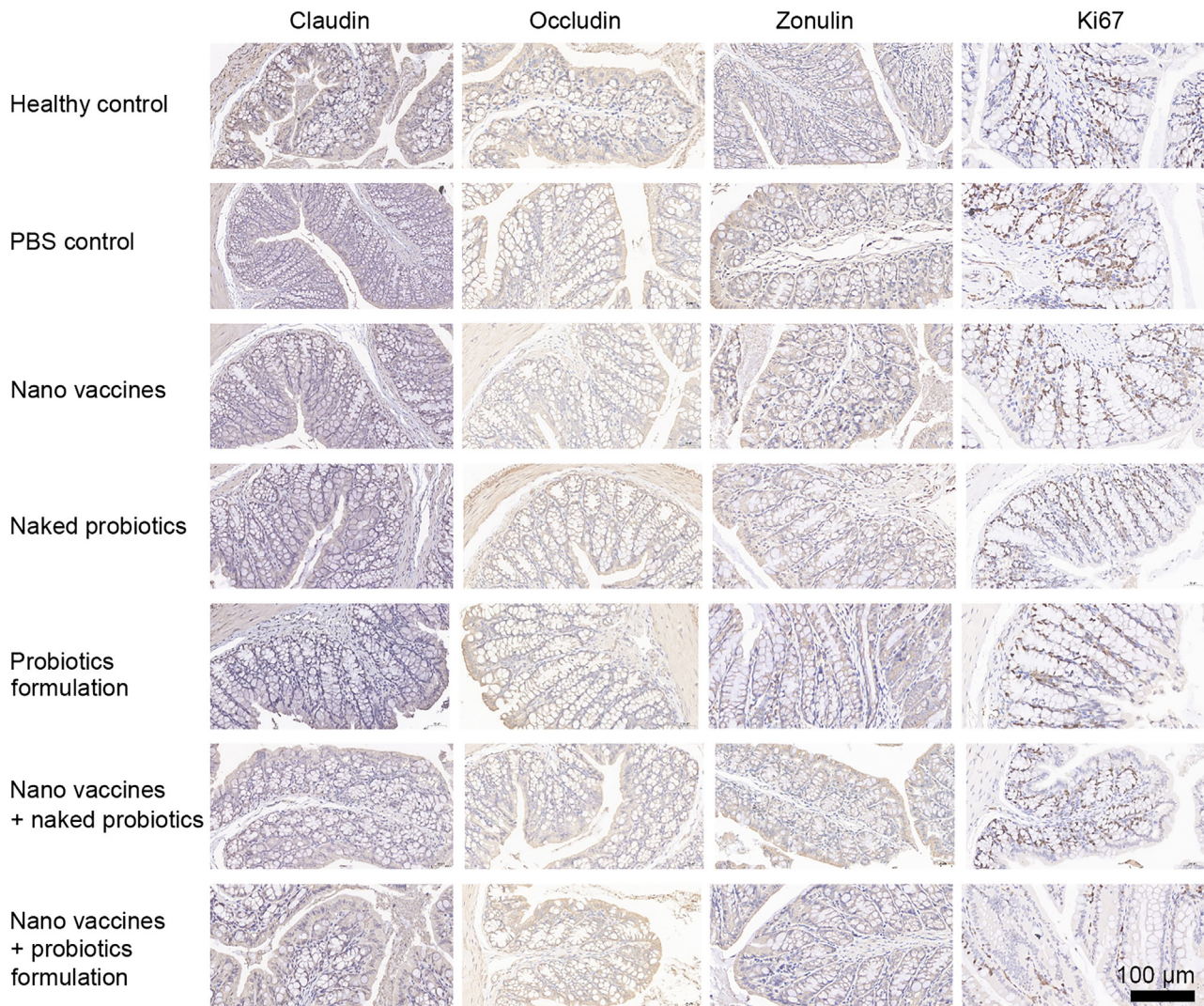


**Figure 5. IHC staining analysis of claudin, occludin, zonulin and Ki67 after AOM/DSS induction (200 $\times$ , scale bar: 100  $\mu$ m)**

intercellular spaces. The mucus layer enables GC to fight against exogenous invasion,<sup>34</sup> GCs also receive and participate in immune regulation.<sup>35</sup> To investigate the integrity of the intestinal epithelial barrier in mice, the presence of mucin-producing goblet cells in colon tissue was analyzed. The results showed that, after AB/PAS staining, the colonic goblet cells in the mice treated with probiotics formulation or nanovaccines + probiotics formulation were significantly increased compared to other groups (Figure 4). It was found that the mice treated with nanovaccines + probiotics formulation contained the richest abundance of colonic goblet cells. The results further illustrated that the co-administration of nanovaccines and probiotics formulation could enhance the resistance to AOM/DSS-induced colon cancer by maintaining the integrity of the epithelial tissue (Figure 4).

To further examine the integrity of the mouse intestinal epithelial system, intestinal tight junction proteins (Claudin-3 [CLDN3], Zonulin and occludin) and colonic epithelial cell proliferation (Ki-67<sup>+</sup> cells) were further studied. Among them, the reduction or redistribution of claudin-3 is associated with increased intestinal permeability,<sup>36</sup> and occludin is a protein component of tight junctions, the removal or reduced expression of it will lead to loss of the intestinal barrier, that is, the lower the occludin, the more permeable the gut is.<sup>37,38</sup> Zonulin family peptides (zonulin) are potent regulators of tight junctions in the gut, and zonulin levels are positively correlated with gut permeability.<sup>39,40</sup> The results showed that the proportion of positive cells

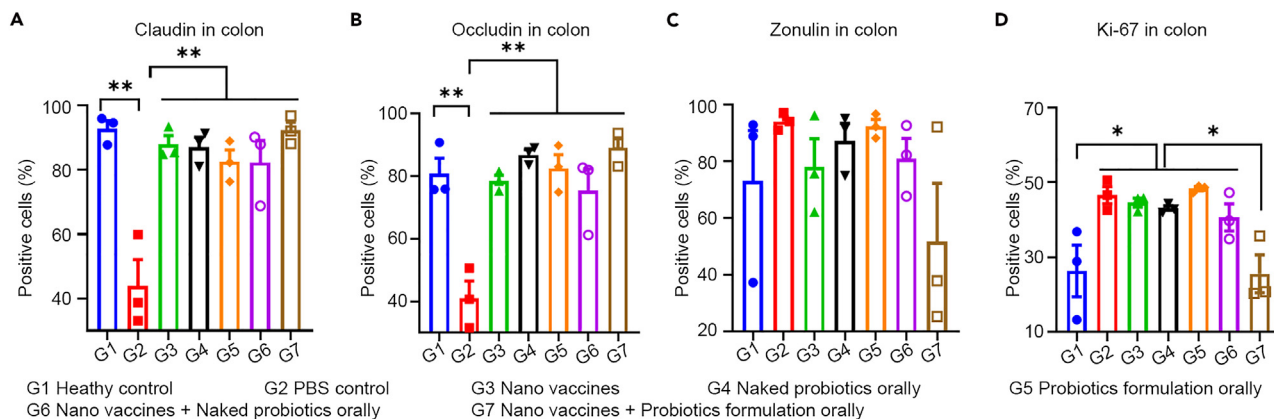


**Figure 6. Immunohistochemical analysis of tight junction protein in colon**

(A) Analysis of the proportion of claudin-positive cells in colon after AOM/DSS induction.

(B) Analysis of the proportion of occludin-positive cells in colon after AOM/DSS induction.

(C) Analysis of the proportion of zonulin-positive cells in colon after AOM/DSS induction.

(D) Analysis of the proportion of Ki-67 positive cells in colon after AOM/DSS induction (n = 3). \* Means significant difference and  $p \leq 0.05$ ; \*\* means significant difference and  $p \leq 0.01$ .

of CLDN3 and occludin in probiotics and/or nanovaccines treated groups was higher than that in the PBS control group (Figures 5 and 6). Furthermore, the proportion of Zonulin, in the nanovaccines + probiotics formulation group was lower than that in the control groups. The analysis of colonic epithelial cell proliferation revealed that nanovaccines + probiotics formulation group led to less cell proliferation than control group (Figures 5 and 6). The above data proved that treatment with nanovaccines + probiotics formulation induced a resistance to primary colon cancer occurrence due to the enhancement of the intestinal tight junction barrier.

### Probiotics treatment efficiently inhibited the tumor growth in vivo

The synergetic effects of probiotics and cancer nanovaccines were evaluated in treating colon cancer, which is shown Figure 7. Results showed that in the oral administration groups, probiotics (formulated or not), nanovaccines and their combinations all could suppress tumor growth and prolong the survival period of mice. Combined nanovaccines with orally administrated probiotics formulation showed synergistic effect and significantly extended the survival period of mice compared to nanovaccines with naked probiotics and other single treatment groups (Figures 7C and 7D). In the intratumoral administration group, combined therapies exhibited better tumor suppression effect and longer survival period than single treatment (Figures 7E and 7F). The combination of nanovaccines with probiotics formulation showed better efficacy than nanovaccines combined with naked probiotics. The synergistic effect indicated that the probiotics formulation prepared in this study could enhance the efficacy of cancer nanovaccines.

### Administration of probiotics formulation increased antigen-specific T cells

To declare the immune specificity toward tumor, the amounts of T cells that specifically recognized tumor antigens in the peripheral immune organs and tumor tissues of mice were explored. Tumor antigen-specific T cells could be activated by tumor antigens and secrete IFN- $\gamma$  after recognizing tumor antigens. The proportion of CD4<sup>+</sup> or CD8<sup>+</sup> T cells that secreted IFN- $\gamma$  after co-incubation with tumor antigens showed that tumor-specific CD4<sup>+</sup> T cells and CD8<sup>+</sup> T cells in nanovaccines group, naked bacterial group and probiotics formulation group significantly increased compared to that PBS group (Figures 8A and 8B); and tumor-specific CD4<sup>+</sup> T cells and CD8<sup>+</sup> T cells in probiotics formulation group increased more than that in naked bacteria group. In addition, free soluble metabolites of probiotics can not efficiently stimulate tumor antigen-specific T cells. Tumor-specific CD8<sup>+</sup> T cells and CD4<sup>+</sup> T cells were further increased when combining nanovaccines with probiotics formulation, which indicated the synergistic immune effects induced by such combination therapy strategy (Figures 8A and 8B). Furthermore, when applying OVA as a marker antigen to label the cancer cells, it was witnessed that both probiotics formulation and nanovaccines can stimulate antigen-specific T cells recognizing OVA peptides (either MHC I restricted OVA<sub>257-264</sub> or MHC II restricted OVA<sub>323-339</sub>); and combining probiotics formulation with nanovaccines showed synergistic effect and further

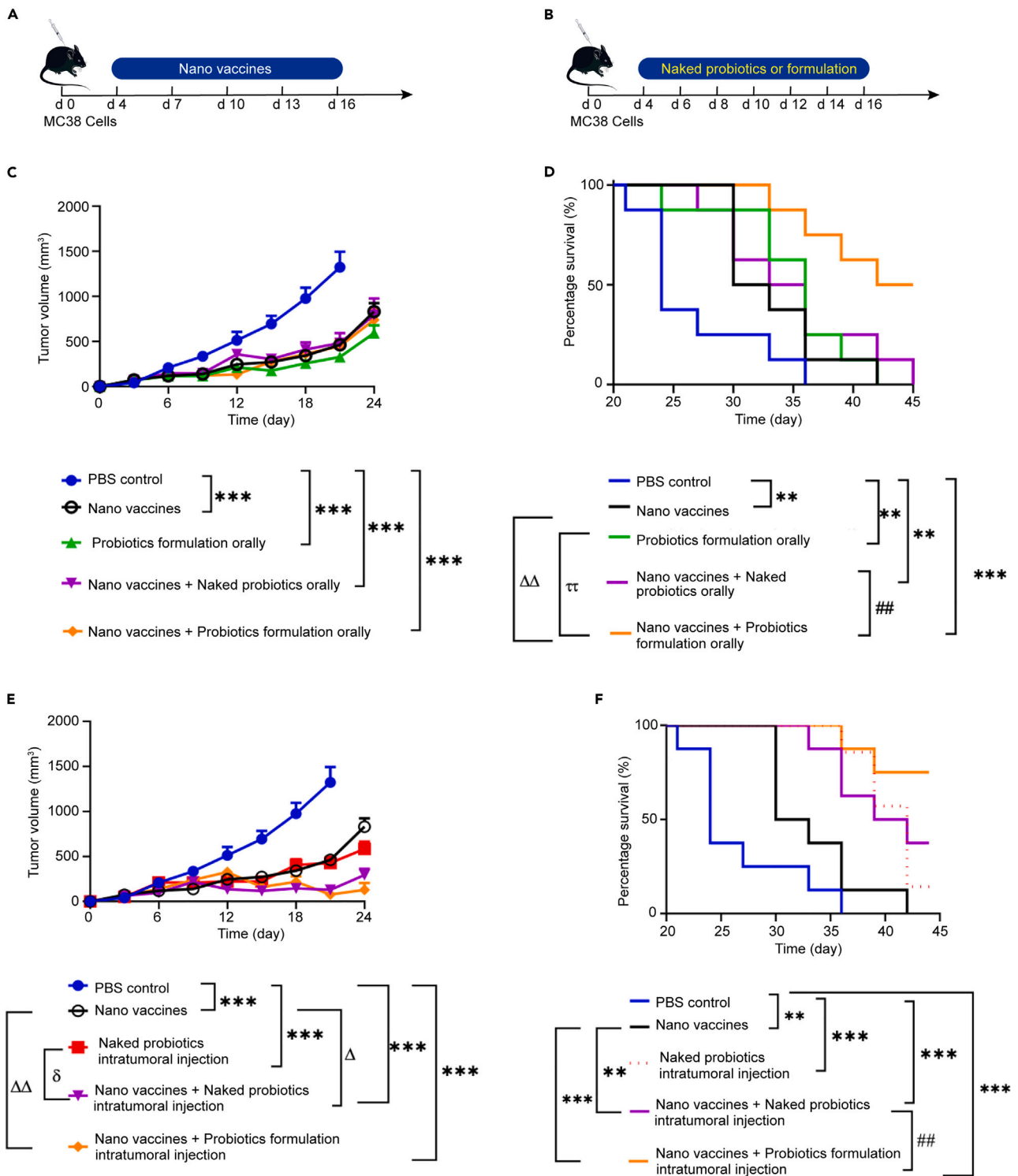


**Figure 7. Probiotics formulation combined with cancer nanovaccine suppressed the growth of MC38 colon tumor**

(A) Treatment strategy of nanovaccines for colon cancer bearing mice.

(B) Treatment strategy of naked or formulated probiotics for colon cancer bearing mice.

**Figure 7. Continued**

(C and D) Tumor growth curves and survival curves of mice treated with oral probiotics formulation and/or subcutaneous injection of nanovaccines (n = 8). (E and F) Tumor growth curves and survival curves of mice when treated with intratumoral injection of probiotics formulation and/or subcutaneous injection of nanovaccines (n = 8). \*,  $\delta$  and  $\Delta$  means significant difference and  $p \leq 0.05$ ; \*\*,  $\Delta\Delta$ ,  $\tau\tau$  and  $\#\#$  means significant difference and  $p \leq 0.01$ ; \*\*\* means significant difference and  $p \leq 0.005$ .

induced more OVA peptide antigen-specific T cells (Figure S3). This was correlated with the immunotherapy results shown in Figure 7.

In addition, by analyzing the microenvironment of tumor tissue, it was found that total T cells, CD8<sup>+</sup> T cells, CD4<sup>+</sup> T cells, DCs, NK cells and macrophages are all increased in probiotics formulation group and nanovaccine group in the tumor microenvironment; and probiotics and nanovaccines showed synergistic effect (Figures 8C–8I). In addition, the ratio of T<sub>H</sub>17 to T<sub>reg</sub> increased in probiotics formulation treated and nanovaccine treated group, and probiotics and nanovaccines showed synergistic effect.

**Probiotics' preventive effect against MC38 colon cancer**

In this study, the preventive effect of probiotic formulations on MC38 subcutaneous colon cancer model was investigated by oral/subcutaneous administration of *L. rhamnosus* formulations and *B. longum* formulations. By monitoring the tumor growth and survival time (Figure 9), it was found that, compared to the control group, oral and subcutaneous injection of probiotics had a potent preventive efficacy. The efficacy of prolonging the survival time could be further improved by combining with nanovaccines. These data demonstrated that probiotics, either administered orally or subcutaneously, could improve the preventive efficacy of cancer nanovaccines.

**Toxicity study**

The body weight change of MC38 tumor-bearing mice treated with probiotics formulations (either orally or subcutaneously injected) and nanovaccines in therapeutic and preventive studies were shown in Figures S4 and S5. Compared with the PBS group, the body weight of mice in other treatment groups barely showed reduction during the administration period, revealing the satisfactory biosafety of probiotics formulation.

To further investigate the potential toxicity of the probiotic formulation, mice, preventative treated with probiotic formulations and/or nanovaccines, were sacrificed, and then hearts, liver, spleen, lung, and kidney were collected and analyzed by H&E staining. For cardiac tissue sections, there was no significant difference between the healthy control group and the probiotics formulation groups, indicating that there was no obvious cardiotoxicity after treatment with probiotics formulation and nanovaccines (Figure S6). For liver tissue, tumor metastasis was seen in the PBS control group compared to normal healthy mice. However, only a small amount of inflammatory cells infiltration was seen in the liver tissue of probiotics formulation and nanovaccines groups with rare distinct pathological changes, indicating no obvious hepatotoxicity after probiotics formulation and nanovaccines treatment (Figure S6). For spleen tissue, there was no significant difference among all the groups (Figure S6). For lung tissue, compared with healthy control mice, only a small amount of inflammatory cells infiltration appeared in the probiotic formulation group and nanovaccines group, illustrating probiotics formulation and nanovaccines treatments barely exhibit toxicity to lung (Figure S6). For kidney tissue, compared with healthy control mice, a few number of casts were formed in the renal tubular lumen of mice in the PBS control group, while no significant changes were observed in the tissues of probiotics formulation group and nanovaccines group, proving that there was no obvious nephrotoxicity after treatment with probiotic formulations and nanovaccines (Figure S6). The above results together demonstrated the favorable safety and less toxicity of probiotic formulations and nanovaccines.

**Conclusion**

Cancer immunotherapy has developed rapidly in recently years and cancer vaccine, especially cancer nanovaccine, is one of the most important methods in cancer immunotherapy or prevention. Cancer vaccines play their roles by activating tumor-antigen-specific T cells, which is the major killer of cancer cells. The completely activating of antigen-specific T cells need a few weeks, and substances, that can intervene the activating process, may be applied to improve the efficacy of cancer vaccines and achieve a synergistic effect.

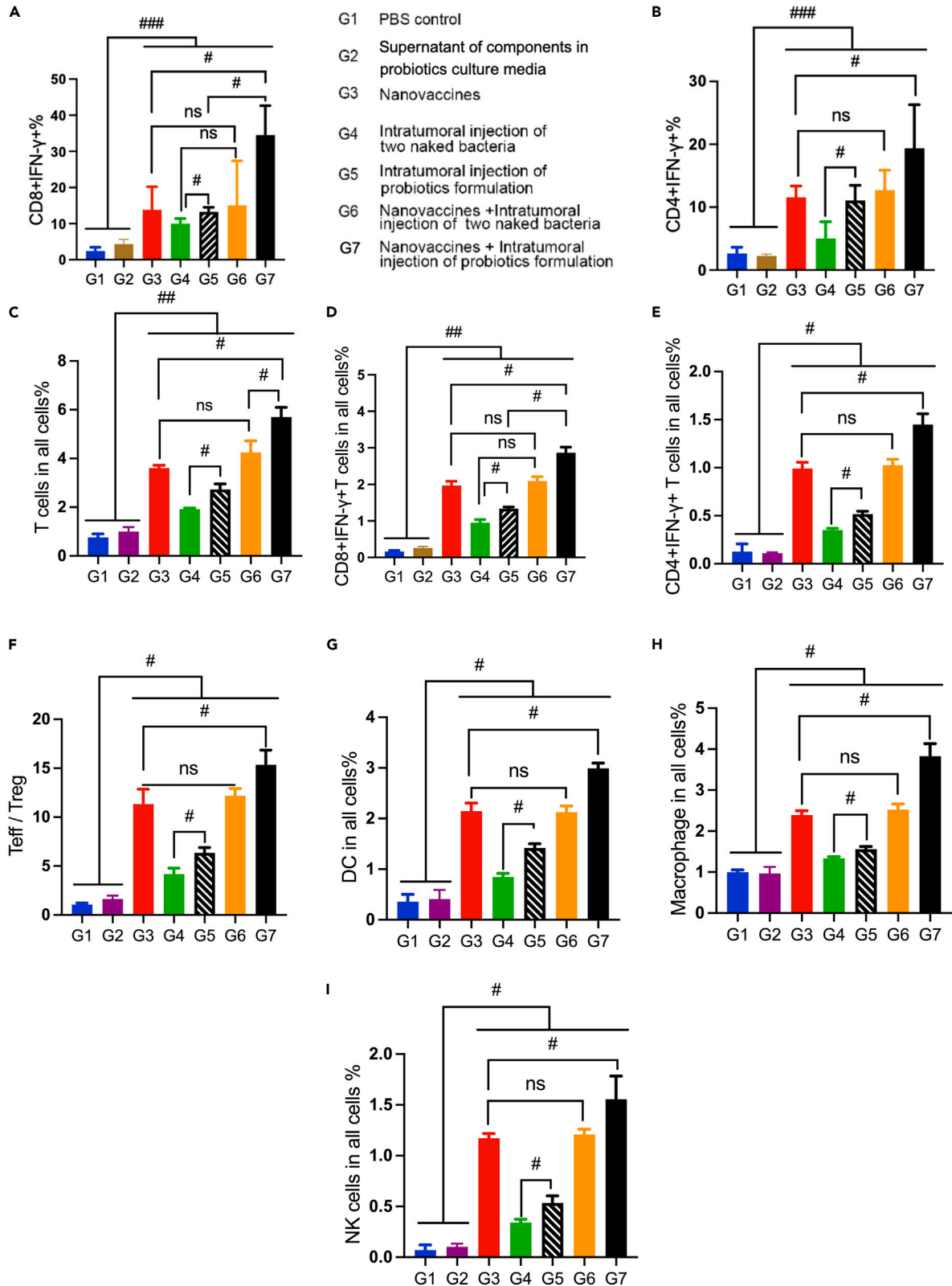


**Figure 8. Analysis of tumor antigen-specific T cells in mouse splenocytes and in tumor microenvironment after treated with probiotics and nanovaccines**

- (A) Flow cytometry analysis of the percentage of IFN- $\gamma$ <sup>+</sup> CD8<sup>+</sup> T cells in splenocytes (n = 3).  
(B) Flow cytometry analysis of IFN- $\gamma$ <sup>+</sup> CD4<sup>+</sup> T cells in splenocytes (n = 3).  
(C) Flow cytometry analysis of the percentage of total T cells in all tumor tissue cells (n = 3).  
(D) Flow cytometry analysis of the percentage of CD8<sup>+</sup> IFN- $\gamma$ <sup>+</sup> cells in all tumor tissue cells (n = 3).  
(E) Flow cytometry analysis of the percentage of CD4<sup>+</sup> IFN- $\gamma$ <sup>+</sup> T cells in all tumor tissue cells (n = 3).  
(F) Analysis of the ratio of T<sub>eff</sub> (CD3<sup>+</sup> CD8<sup>+</sup>) over T<sub>reg</sub> (CD3<sup>+</sup> CD25<sup>+</sup> FOXP3<sup>+</sup>) in all tumor tissue cells (n = 3).  
(G) Flow cytometry analysis of the percentage of DC in all tumor tissue cells (n = 3).  
(H) Flow cytometry analysis of the percentage of macrophages in all tumor tissue cells (n = 3).  
(I) Flow cytometry analysis of the percentage of NK cells in all tumor tissue cells (n = 3). # means significant difference and p ≤ 0.05; ## means significant difference and p ≤ 0.01; ### means significant difference and p ≤ 0.005.

Cancer vaccines provide the antigens for specific immune responses activation, whereas, probiotics may facilitate the cancer immunotherapy and cancer prevention by adjusting body immune homeostasis and activating the innate immune responses, followed by prompting the stimulation of adaptive immune systems. Thus, probiotics can be applied as immune adjuvants to assist the activation of antigen-specific immune responses. However, naked probiotics are limited in stimulating potent immune responses due to the physicochemical characteristics of gastrointestinal tract, and thus proper formulation is needed to maximize the function of probiotics.

In this study, we modified probiotics by coating with lipid membrane, to improve the colonization ability and viability of probiotics. In the colon cancer (CRC) mouse model, either subcutaneous transplanted colon cancer model or chemical induced orthotopic colon cancer model, probiotics formulation alone showed effective preventive and therapeutic efficacy. When probiotics formulation was combined with cancer nanovaccines, the preventive and therapeutic efficacy was significantly improved, and such effects were seen when administered both orally or through subcutaneously (intratumoral) injection. These fully supported that probiotics formulation can be applied alone to treat cancer or applied as an immune adjuvants to improve the efficacy of cancer vaccines.

In the study of preventing chemical-induced orthotopic colon cancer, probiotics formulation efficiently reduced tumor number induced by chemicals in colon, and improved the efficacy of cancer nanovaccines, and the increased tumor-specific T cells demonstrated an enhancement of recognizing and killing cancer cells by this combination strategy. Furthermore, probiotics formulation altered the microenvironment in colon, increased the amounts of goblet cells and expression of protective proteins, such as claudin and occluding, thus might protect the colon from intruding of cancer cells. All in all, the studies demonstrated a probiotics formulation that can be applied in cancer prevention and immunotherapy, especially work together with cancer nanovaccines to achieve a better efficacy.

**Limitations of the study**

In the studies of intratumoral injection of probiotics formulation, further deeper investigations can be conducted. For instances, bacteria facilitate the immune responses by staying outside of cancer cells or penetrating into cancer cells need to be further investigated systematically.

**STAR★METHODS**

Detailed methods are provided in the online version of this paper and include the following:

- [KEY RESOURCES TABLE](#)
- [RESOURCE AVAILABILITY](#)
  - Lead contact
  - Materials availability
  - Data and code availability
- [EXPERIMENTAL MODEL AND SUBJECT DETAILS](#)
  - Animals and ethics statement
  - Probiotics applied in the studies
  - Cell lines
  - Declaration
- [METHOD DETAILS](#)

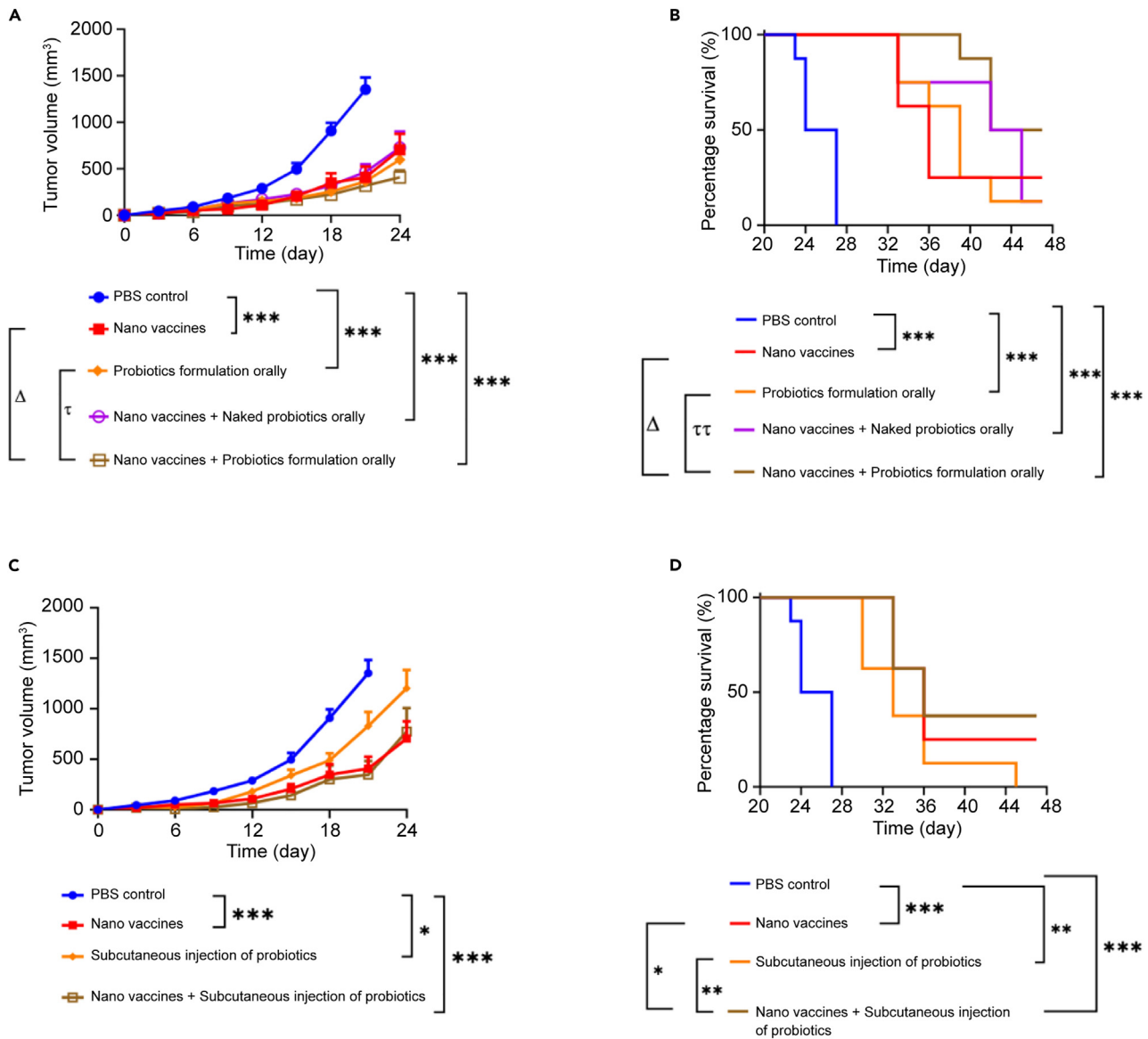


**Figure 9. Comparison of the efficacy of probiotics formulations (oral or subcutaneous injection) and nanovaccines (subcutaneous injection) in preventing MC38 colon cancer**

(A and B) Tumor growth curves and mouse survival curves of mice prevented by orally administered probiotics formulation and subcutaneously injected nanovaccines (n = 8).

(C and D) Tumor growth curves and mouse survival curves of mice prevented by subcutaneous injection of probiotics and nanovaccines (n = 8). \* Means significant difference and  $p \leq 0.05$ ; \*\* means significant difference and  $p \leq 0.01$ ; \*\*\* means significant difference and  $p \leq 0.005$ .

- Preparation of probiotics formulation
- Characterization of probiotics formulation
- Growth curves of probiotics formulation
- Cell viability investigation of coated bacteria
- Stability of probiotics formulation in simulated gastrointestinal tract (GI) fluids
- Preparation and characterization of cancer nanovaccines reassembled from tumor tissue of MC38 colon cancer
- Immunotherapy of colon cancer by NV
- Prevention of colon cancers by NV
- *In vivo* colonization experiments

- Prevention of orthotopic colon cancer
- Investigation of microenvironment of colon samples
- *In vivo* anti-cancer therapeutic evaluation
- Analysis of tumor antigen-specific T cells in splenocytes of treated mice
- Analysis of the tumor infiltrating lymphocyte populations
- Prevention of colon cancer in subcutaneous cancer mouse model
- **QUANTIFICATION AND STATISTICAL ANALYSIS**

## SUPPLEMENTAL INFORMATION

Supplemental information can be found online at <https://doi.org/10.1016/j.isci.2023.107167>.

## ACKNOWLEDGMENTS

The studies were supported by Suzhou Ersheng Biopharmaceutical Co., Ltd, Suzhou, People's Republic of China, Priority Academic Program Development (PAPD) of Jiangsu Higher Education Institutions and Jiangsu Province Engineering Research Center of Precision Diagnostics and Therapeutics Development, Soochow University, Suzhou 215123, China.

## AUTHOR CONTRIBUTIONS

M.L. conceived and designed the study. M.Z., X.X., L.D., L.M., M.X., and S.N. contribute to conducting the investigation; M.L., Y.W., and F.M. contributed to resources of the studies. X.X., M.Z., F.M., L.D., M.C., and X.L. contribute to analysis of data and drawing the figures. X.X., M.L., and L.D. contribute to writing the manuscript, X.X. and M.L. revised the manuscript.

## DECLARATION OF INTERESTS

M.L. is a shareholder of Suzhou Ersheng Biopharmaceutical Co., Ltd, Suzhou, People's Republic of China. M.L. has applied a patent related to this study. The remaining authors have reported no financial interests or potential conflicts of interest.

Received: February 2, 2023

Revised: April 26, 2023

Accepted: June 13, 2023

Published: June 19, 2023

## REFERENCES

1. Labianca, R., Beretta, G.D., Kildani, B., Milesi, L., Merlin, F., Mosconi, S., Pessi, M.A., Prochilo, T., Quadri, A., Gatta, G., et al. (2010). Colon cancer. *Crit. Rev. Oncol. Hematol.* 74, 106–133. <https://doi.org/10.1016/j.critrevonc.2010.01.010>.
2. Taghizadeh, H., and Prager, G.W. (2020). Personalized Adjuvant Treatment of Colon Cancer. *Visc. Med.* 36, 397–406. <https://doi.org/10.1159/000508175>.
3. Sung, H., Ferlay, J., Siegel, R.L., Laversanne, M., Soerjomataram, I., Jemal, A., and Bray, F. (2021). Global Cancer Statistics 2020: GLOBOCAN Estimates of Incidence and Mortality Worldwide for 36 Cancers in 185 Countries. *Ca - Cancer J. Clin.* 71, 209–249. <https://doi.org/10.3322/caac.21660>.
4. Page, A.J., Cosgrove, D.C., Herman, J.M., and Pawlik, T.M. (2015). Advances in understanding of colorectal liver metastasis and implications for the clinic. *Expert Rev. Gastroenterol. Hepatol.* 9, 245–259. <https://doi.org/10.1586/17474124.2014.940897>.
5. Gao, J., Logan, K.A., Nesbitt, H., Callan, B., McKaig, T., Taylor, M., Love, M., McHale, A.P., Griffith, D.M., and Callan, J.F. (2021). A single microbubble formulation carrying 5-fluorouridine, Irinotecan and oxaliplatin to enable FOLFIRINOX treatment of pancreatic and colon cancer using ultrasound targeted microbubble destruction. *J. Contr. Release* 338, 358–366. <https://doi.org/10.1016/j.jconrel.2021.08.050>.
6. Czito, B.G., Bendell, J., and Willett, C.G. (2006). Radiation therapy for resectable colon cancer. Is there a role in the modern chemotherapy era? *Oncology (Williston Park)* 20, 179–187.
7. Willyard, C. (2021). The colon cancer conundrum. *Nature*. <https://doi.org/10.1038/d41586-021-03405-6>.
8. Ravensbergen, C.J., Polack, M., Roelands, J., Crobach, S., Putter, H., Gelderblom, H., Tollenaar, R., and Mesker, W.E. (2021). Combined assessment of the tumor-stroma ratio and tumor immune cell infiltrate for immune checkpoint inhibitor therapy response prediction in colon cancer. *Cells* 10, 2935. <https://doi.org/10.3390/cells10112935>.
9. Huang, W., He, L., Zhang, Z., Shi, S., and Chen, T. (2021). Shape-Controllable Tellurium-Driven Heterostructures with Activated Robust Immunomodulatory Potential for Highly Efficient Radiophothermal Therapy of Colon Cancer. *ACS Nano* 15, 20225–20241. <https://doi.org/10.1021/acsnano.1c08237>.
10. Noshio, K., Sukawa, Y., Adachi, Y., Ito, M., Mitsuhashi, K., Kurihara, H., Kanno, S., Yamamoto, I., Ishigami, K., Igarashi, H., et al. (2016). Association of fusobacterium nucleatum with immunity and molecular alterations in colorectal cancer. *World J. Gastroenterol.* 22, 557–566. <https://doi.org/10.3748/wjg.v22.i2.557>.
11. Xing, C., Wang, M., Ajibade, A.A., Tan, P., Fu, C., Chen, L., Zhu, M., Hao, Z.Z., Chu, J., Yu, X., et al. (2021). Microbiota regulate innate immune signaling and protective immunity against cancer. *Cell Host Microbe* 29, 959–974.e7. <https://doi.org/10.1016/j.chom.2021.03.016>.
12. Gu, Y., Chen, Y., Wei, L., Wu, S., Shen, K., Liu, C., Dong, Y., Zhao, Y., Zhang, Y., Zhang, C., et al. (2021). ABHD5 inhibits YAP-induced

- c-Met overexpression and colon cancer cell stemness via suppressing YAP methylation. *Nat. Commun.* 12, 6711. <https://doi.org/10.1038/s41467-021-26967-5>.
13. Nelson, M.H., Diven, M.A., Huff, L.W., and Paulos, C.M. (2015). Harnessing the microbiome to enhance cancer immunotherapy. *J. Immunol. Res.* 2015, 368736. <https://doi.org/10.1155/2015/368736>.
  14. Routy, B., Gopalakrishnan, V., Daillère, R., Zitvogel, L., Wargo, J.A., and Kroemer, G. (2018). The gut microbiota influences anticancer immunosurveillance and general health. *Nat. Rev. Clin. Oncol.* 15, 382–396. <https://doi.org/10.1038/s41571-018-0006-2>.
  15. Banna, G.L., Torino, F., Marletta, F., Santagati, M., Salemi, R., Cannarozzo, E., Falzone, L., Ferrau, F., and Libra, M. (2017). Lactobacillus rhamnosus GG: An Overview to Explore the Rationale of Its Use in Cancer. *Front. Pharmacol.* 8, 603. <https://doi.org/10.3389/fphar.2017.00603>.
  16. Chang, C.W., Liu, C.Y., Lee, H.C., Huang, Y.H., Li, L.H., Chiau, J.S.C., Wang, T.E., Chu, C.H., Shih, S.C., Tsai, T.H., and Chen, Y.J. (2018). Lactobacillus casei Variety rhamnosus Probiotic Preventively Attenuates 5-Fluorouracil/Oxaliplatin-Induced Intestinal Injury in a Syngeneic Colorectal Cancer Model. *Front. Microbiol.* 9, 983. <https://doi.org/10.3389/fmicb.2018.00983>.
  17. Dehghani, N., Tafvizi, F., and Jafari, P. (2021). Cell cycle arrest and anti-cancer potential of probiotic Lactobacillus rhamnosus against HT-29 cancer cells. *Bioimpacts* 11, 245–252. <https://doi.org/10.34172/bi.2021.32>.
  18. Rahimi, A.M., Nabavizadeh, F., Ashabi, G., Halimi, S., Rahimpour, M., Vahedian, J., and Panahi, M. (2021). Probiotic Lactobacillus rhamnosus Supplementation Improved Capecitabine Protective Effect against Gastric Cancer Growth in Male BALB/c Mice. *Nutr. Cancer* 73, 2089–2099. <https://doi.org/10.1080/01635581.2020.1832237>.
  19. Vivarelli, S., Salemi, R., Candido, S., Falzone, L., Santagati, M., Stefani, S., Torino, F., Banna, G.L., Tonini, G., and Libra, M. (2019). Gut microbiota and cancer: From pathogenesis to therapy. *Cancers* 11, 38. <https://doi.org/10.3390/cancers11010038>.
  20. Kandasamy, M., Bay, B.H., Lee, Y.K., and Mahendran, R. (2011). Lactobacilli secreting a tumor antigen and IL15 activates neutrophils and dendritic cells and generates cytotoxic T lymphocytes against cancer cells. *Cell. Immunol.* 271, 89–96. <https://doi.org/10.1016/j.cellimm.2011.06.004>.
  21. Sun, S., Luo, L., Liang, W., Yin, Q., Guo, J., Rush, A.M., Lv, Z., Liang, Q., Fischbach, M.A., Sonnenburg, J.L., et al. (2020). Bifidobacterium alters the gut microbiota and modulates the functional metabolism of T regulatory cells in the context of immune checkpoint blockade. *Proc. Natl. Acad. Sci. USA* 117, 27509–27515. <https://doi.org/10.1073/pnas.1921223117>.
  22. Ding, W.K., and Shah, N.P. (2007). Acid, bile, and heat tolerance of free and microencapsulated probiotic bacteria. *J. Food Sci.* 72, M446–M450. <https://doi.org/10.1111/j.1750-3841.2007.00565.x>.
  23. Anselmo, A.C., McHugh, K.J., Webster, J., Langer, R., and Jaklenec, A. (2016). Layer-by-Layer Encapsulation of Probiotics for Delivery to the Microbiome. *Adv. Mater.* 28, 9486–9490. <https://doi.org/10.1002/adma.201603270>.
  24. Li, Z., Behrens, A.M., Ginat, N., Tzeng, S.Y., Lu, X., Sivan, S., Langer, R., and Jaklenec, A. (2018). Biofilm-Inspired encapsulation of probiotics for the treatment of complex infections. *Adv. Mater.* 30, e1803925. <https://doi.org/10.1002/adma.201803925>.
  25. Chen, W., Wang, Y., Qin, M., Zhang, X., Zhang, Z., Sun, X., and Gu, Z. (2018). Bacteria-driven hypoxia targeting for combined biotherapy and photothermal therapy. *ACS Nano* 12, 5995–6005. <https://doi.org/10.1021/acsnano.8b02235>.
  26. Cao, Z., Cheng, S., Wang, X., Pang, Y., and Liu, J. (2019). Camouflaging bacteria by wrapping with cell membranes. *Nat. Commun.* 10, 3452. <https://doi.org/10.1038/s41467-019-11390-8>.
  27. Qiao, Y., Yang, F., Xie, T., Du, Z., Zhong, D., Qi, Y., Li, Y., Li, W., Lu, Z., Rao, J., et al. (2020). Engineered algae: A novel oxygen-generating system for effective treatment of hypoxic cancer. *Sci. Adv.* 6, eaba5996. <https://doi.org/10.1126/sciadv.aba5996>.
  28. Hu, Q., Wu, M., Fang, C., Cheng, C., Zhao, M., Fang, W., Chu, P.K., Ping, Y., and Tang, G. (2015). Engineering nanoparticle-coated bacteria as oral DNA vaccines for cancer immunotherapy. *Nano Lett.* 15, 2732–2739. <https://doi.org/10.1021/acs.nanolett.5b00570>.
  29. Harimoto, T., Hahn, J., Chen, Y.Y., Im, J., Zhang, J., Hou, N., Li, F., Coker, C., Gray, K., Harr, N., et al. (2022). A programmable encapsulation system improves delivery of therapeutic bacteria in mice. *Nat. Biotechnol.* 40, 1259–1269. <https://doi.org/10.1038/s41587-022-01244-y>.
  30. Cao, Z., Wang, X., Pang, Y., Cheng, S., and Liu, J. (2019). Biointerfacial self-assembly generates lipid membrane coated bacteria for enhanced oral delivery and treatment. *Nat. Commun.* 10, 5783. <https://doi.org/10.1038/s41467-019-13727-9>.
  31. Wang, L., Cao, Z., Zhang, M., Lin, S., and Liu, J. (2022). Spatiotemporally Controllable Distribution of Combination Therapeutics in Solid Tumors by Dually Modified Bacteria. *Adv. Mater.* 34, e2106669. <https://doi.org/10.1002/adma.202106669>.
  32. Ma, L., Diao, L., Peng, Z., Jia, Y., Xie, H., Li, B., Ma, J., Zhang, M., Cheng, L., Ding, D., et al. (2021). Immunotherapy and Prevention of Cancer by Nanovaccines Loaded with Whole-Cell Components of Tumor Tissues or Cells. *Adv. Mater.* 33, e2104849. <https://doi.org/10.1002/adma.202104849>.
  33. Diao, L., Ma, L., Cheng, J., Pan, Y., Peng, Z., Zhang, L., Xu, M., Li, Y., Zhang, X., Jiang, H., et al. (2022). Across-cancer specific immune responses induced by nanovaccines or microvaccines to prevent different cancers and cancer metastasis. *iScience* 25, 105511. <https://doi.org/10.1016/j.isci.2022.105511>.
  34. Johansson, M.E.V., and Hansson, G.C. (2016). Immunological aspects of intestinal mucus and mucins. *Nat. Rev. Immunol.* 16, 639–649. <https://doi.org/10.1038/nri.2016.88>.
  35. Pelaseyed, T., Bergström, J.H., Gustafsson, J.K., Ermund, A., Birchenough, G.M.H., Schütte, A., van der Post, S., Svensson, F., Rodríguez-Piñero, A.M., Nyström, E.E.L., et al. (2014). The mucus and mucins of the goblet cells and enterocytes provide the first defense line of the gastrointestinal tract and interact with the immune system. *Immunol. Rev.* 260, 8–20. <https://doi.org/10.1111/imr.12182>.
  36. Ling, X., Linglong, P., Weixia, D., and Hong, W. (2016). Protective effects of bifidobacterium on intestinal barrier function in LPS-induced enterocyte barrier injury of Caco-2 monolayers and in a rat NEC model. *PLoS One* 11, e0161635. <https://doi.org/10.1371/journal.pone.0161635>.
  37. Kuo, W.T., Shen, L., Zuo, L., Shashikanth, N., Ong, M., Wu, L., Zha, J., Edelblum, K.L., Wang, Y., Wang, Y., et al. (2019). Inflammation-induced occludin downregulation limits epithelial apoptosis by suppressing caspase-3 expression. *Gastroenterology* 157, 1323–1337. <https://doi.org/10.1053/j.gastro.2019.07.058>.
  38. Liu, Y., Gong, Z., Zhou, J., Yan, J., and Cai, W. (2021). Lin 28A/occludin axis: An aberrantly activated pathway in intestinal epithelial cells leading to impaired barrier function under total parenteral nutrition. *Faseb. J.* 35, e21189. <https://doi.org/10.1096/fj.202001819R>.
  39. Sturgeon, C., and Fasano, A. (2016). Zonulin, a regulator of epithelial and endothelial barrier functions, and its involvement in chronic inflammatory diseases. *Tissue Barriers* 4, e1251384. <https://doi.org/10.1080/21688370.2016.1251384>.
  40. Stevens, B.R., Goel, R., Seungbum, K., Richards, E.M., Holbert, R.C., Pepine, C.J., and Raizada, M.K. (2018). Increased human intestinal barrier permeability plasma biomarkers zonulin and FAP2 correlated with plasma LPS and altered gut microbiome in anxiety or depression. *Gut* 67, 1555–1557. <https://doi.org/10.1136/gutjnl-2017-314759>.
  41. Shukla, S., and Bajpai, V.K. (2017). Visual demonstration of transmission electron microscopy for intracellular observation of a single bacterial cell. *Bangladesh J. Pharmacol.* 12, 23. <https://doi.org/10.3329/bjp.v12i1.31390>.
  42. Bader, J.E., Enos, R.T., Velázquez, K.T., Carson, M.S., Nagarkatti, M., Nagarkatti, P.S., Chatzistamou, I., Davis, J.M., Carson, J.A., Robinson, C.M., and Murphy, E.A. (2018). Macrophage depletion using clodronate liposomes decreases tumorigenesis and alters gut microbiota in the AOM/DSS mouse model of colon cancer. *Am. J. Physiol. Gastrointest. Liver Physiol.* 314, G22–G31. <https://doi.org/10.1152/ajpgi.00229.2017>.

43. Ostman, S., Rask, C., Wold, A.E., Hultkrantz, S., and Telemo, E. (2006). Impaired regulatory T cell function in germ-free mice. *Eur. J. Immunol.* 36, 2336–2346. <https://doi.org/10.1002/eji.200535244>.
44. Bertocchi, A., Carloni, S., Ravenda, P.S., Bertalot, G., Spadoni, I., Lo Cascio, A., Gandini, S., Lizier, M., Braga, D., Asnicar, F., et al. (2021). Gut vascular barrier impairment leads to intestinal bacteria dissemination and colorectal cancer metastasis to liver. *Cancer Cell* 39, 708–724.e11. <https://doi.org/10.1016/j.ccell.2021.03.004>.
45. De Robertis, M., Massi, E., Poeta, M.L., Carotti, S., Morini, S., Cecchetelli, L., Signori, E., and Fazio, V.M. (2011). The AOM/DSS murine model for the study of colon carcinogenesis: From pathways to diagnosis and therapy studies. *J. Carcinog.* 10, 9. <https://doi.org/10.4103/1477-3163.78279>.
46. Overacre-Delgoffe, A.E., Bumgarner, H.J., Cillo, A.R., Burr, A.H.P., Tometch, J.T., Bhattacharjee, A., Bruno, T.C., Vignali, D.A.A., and Hand, T.W. (2021). Microbiota-specific T follicular helper cells drive tertiary lymphoid structures and anti-tumor immunity against colorectal cancer. *Immunity* 54, 2812–2824.e4. <https://doi.org/10.1016/j.immuni.2021.11.003>.
47. Erben, U., Loddenkemper, C., Doerfel, K., Spieckermann, S., Haller, D., Heimesaat, M.M., Zeitz, M., Siegmund, B., and Kühl, A.A. (2014). A guide to histomorphological evaluation of intestinal inflammation in mouse models. *Int. J. Clin. Exp. Pathol.* 7, 4557–4576.
48. Yakkundi, P., Gonsalves, E., Galou-Lameyer, M., Selby, M.J., and Chan, W.K. (2019). Aryl hydrocarbon receptor acts as a tumor suppressor in a syngeneic MC38 colon carcinoma tumor model. *Hypoxia* 7, 1–16. <https://doi.org/10.2147/HP.S196301>.
49. Hos, B.J., Camps, M.G.M., van den Bulk, J., Tondini, E., van den Ende, T.C., Ruano, D., Franken, K., Janssen, G.M.C., Ru, A., Filippov, D.V., et al. (2019). Identification of a neo-epitope dominating endogenous CD8 T cell responses to MC-38 colorectal cancer. *OncolImmunology* 9, 1673125. <https://doi.org/10.1080/2162402X.2019.1673125>.
50. Grasselly, C., Denis, M., Bourguignon, A., Talhi, N., Mathe, D., Tourette, A., Serre, L., Jordheim, L.P., Matera, E.L., and Dumontet, C. (2018). The Antitumor Activity of Combinations of Cytotoxic Chemotherapy and Immune Checkpoint Inhibitors Is Model-Dependent. *Front. Immunol.* 9, 2100. <https://doi.org/10.3389/fimmu.2018.02100>.

STAR★METHODS

KEY RESOURCES TABLE

REAGENT or RESOURCE	SOURCE	IDENTIFIER
<b>Antibodies</b>		
PE anti-mouse CD8a Antibody	BioLegend	Cat. # 100708 AB_312747
APC anti-mouse/human CD45R/B220 Antibody	BioLegend	Cat. # 103212 AB_312997
APC/Cyanine7 anti-mouse F4/80 Antibody	BioLegend	Cat. # 123118 AB_893477
PerCP/Cyanine5.5 anti-mouse CD11c Antibody	BioLegend	Cat. # 117328 AB_2129641
APC-Cyanine7-anti-mouse CD3 Antibody	BioLegend	Cat. # 100222 AB_2242784
FITC-anti-mouse CD4 Antibody	BioLegend	Cat. #130308 AB_1279237
PE/Cyanine7 anti-mouse CD4 Antibody	BioLegend	Cat. #100422 AB_312707
APC-anti-mouse IFN- $\gamma$ Antibody	BioLegend	Cat. # 505810 AB_315404
Brilliant Violet 421™ anti-mouse FOXP3 Antibody	BioLegend	Cat. # 126419 AB_2565933
PE/Cyanine7 anti-mouse CD49b (pan-NK cells) Antibody	BioLegend	Cat. # 108922 AB_2561460
FITC anti-mouse CD25 Antibody	BioLegend	Cat. # 101908 AB_961212
TruStain FcX™ (anti-mouse CD16/32) Antibody	BioLegend	Cat. #101320 AB_1574975
Zombie Aqua™ Fixable Viability Kit	BioLegend	Cat. # 423102
<b>Bacterial and virus strains</b>		
<i>Lactobacillus rhamnosus</i>	GUANGDONG HUANKAI MICROBIAL SCI&TECH Co. Ltd	Cat. # ATCC7469
<i>Bifidobacterium longum</i>	GUANGDONG HUANKAI MICROBIAL SCI&TECH Co. Ltd	Cat. # ATCC15697
<b>Chemicals, peptides, and recombinant proteins</b>		
Calcium chloride, anhydrous	Sango Biotech	CAS # 10043-52-4 Cat. # A501330-0500
Cholesterol	Sango Biotech	CAS # 57-88-5 Cat. # A610122-0050
Ampicillin sodium	Sango Biotech	Cat. # A610029-0025
Kanamycin sulfate	Sango Biotech	CAS # 25389-94-0 Cat. # A600286-0005
Neomycin trisulfate salt hydrate	Sango Biotech	CAS #1405-10-3 Cat. # A610366-0025
Metronidazole	Sango Biotech	CAS # 443-48-1 Cat. # A600633-0025
Vancomycin hydrochloride	Sango Biotech	CAS # 1404-93-9 Cat. # A600983-0001
Azoxymethan	sigma-aldrich	CAS # 25843-45-2 Cat. # a5486
Dextran sulfate sodium salt	sigma-aldrich	CAS # 9011-18-1 Cat. # 51227
L- $\alpha$ -Phosphatidyl-DL-glycerol	AVT (Shanghai) Pharmaceutical Tech CO. Ltd	CAS # 62700-69-0 Cat. # S02005
Urea	Thermo scientific	CAS # 57-13-6 Cat. # A12360.36
Poly (vinyl alcohol) (PVA, 26 360627, MW: 9,000–10,000 Da)	Sigma Aldrich	CAS # 9002-89-5 Cat. #360627
Rhodamine B modified PLGA (24K–38K, 50:50)	Xian ruixi Biological Technology Co.,Ltd	Cat. # R-L-38K
(R)-2,3-bis(palmitoyloxy)propyl (2-(trimethylammonio)ethyl) phosphate	AVT (Shanghai) Pharmaceutical Tech CO. Ltd	CAS # 63-89-8 Cat. # S01004
2-distearoyl-sn-glycero-3-phosphoethanolamine-N-[(polyethylene glycol)-2000]-Fluorescein	AVT (Shanghai) Pharmaceutical Tech CO. Ltd	Cat. # F05002

(Continued on next page)

**Continued**

REAGENT or RESOURCE	SOURCE	IDENTIFIER
MRS Broth	Qingdao Hope Bio-Technology CO. Ltd., China	Cat. #HB0384-1
Anaerobic gas producing bag	Qingdao Hope Bio-Technology CO. Ltd., China	Cat. #HBY001
Enhanced Cell Counting Kit-8	Beyotime	Cat. # C0038
Anti -Claudin 3 Mouse mAb	Servicebio	Cat. # GB14069
Anti-Haptoglobin Rabbit pAb	Servicebio	Cat. # GB115437
Anti -Occludin Rabbit pAb	Servicebio	Cat. # GB111401
Anti -Ki67 Rabbit pAb	Servicebio	Cat. # GB111141
Anti -HRP-3 Rabbit pAb	Servicebio	Cat. # GB112199
Anti-HRPT2/Parafibromin Mouse mAb	Servicebio	Cat. # GB14130
Pepsin from Porcine Stomach	aladdin	CAS # 9001-75-6
Trypsin from porcine pancreas	aladdin	CAS # 9002-07-7
CollagenaseIV	solarbio	CAS # 9001-12-1
DeoxyribonucleaseI	solarbio	CAS # 9003-98-9
<b>Experimental models: Cell lines</b>		
MC38 cell line	FuHeng Cell Center , Shanghai, China	Cat. # FH0125
MC38-OVA cell line	FuHeng Cell Center , Shanghai, China	Cat. # FH0126
<b>Experimental models: Organisms/strains</b>		
Mouse: C57BL/6J	CharlesRiver	Cat. # C57BL/6JNifdc
<b>Oligonucleotides</b>		
pGEN-luxCDABE	addgene	Cat. # 44918
poly(I:C) (vac-pic)	InvivoGen	Cat. # tlr-pic-5
<b>Software and algorithms</b>		
FlowJo v10.5.3	BD Biosciences	<a href="https://www.flowjo.com/">https://www.flowjo.com/</a>
GraphPad Prism 8.0	GraphPad	<a href="https://www.graphpad.com">https://www.graphpad.com</a>

**RESOURCE AVAILABILITY****Lead contact**

Further information and requests for resources should be directed to and will be fulfilled by the lead contact, Mi Liu ([mi.liu@suda.edu.cn](mailto:mi.liu@suda.edu.cn)).

**Materials availability**

There are no newly generated materials to report.

**Data and code availability**

The data supporting the findings of this study are included in the paper. All other relevant data are available from the lead corresponding author upon reasonable request. This paper does not report original code. Any additional information required to reanalyze the data reported in this paper is available from the [lead contact](#) upon request.

**EXPERIMENTAL MODEL AND SUBJECT DETAILS****Animals and ethics statement**

6–8 weeks old female C57BL/6 mice (CharlesRiver, Cat. # C57BL/6JNifdc) were used. All the mice were ordered from the animal facility platform of Soochow University. In the pharmaceutical efficacy studies, at least 8 mice were applied in each group, and in other studies at least 3 mice were applied in each group. Mice were allocated to experimental groups randomly. Mice were housed in an animal facility under

constant environmental conditions (room temperature,  $21 \pm 1^\circ\text{C}$ ; relative humidity, 40–70% and a 12 h light-dark cycle). All mice had access to food and water. All animal experiments were carried out following protocols approved by Laboratory Animal Center of Soochow University. All animal work was approved and monitored by the Animal Ethics Committee of Soochow University.

### Probiotics applied in the studies

Two probiotics *Lactobacillus rhamnosus* (Cat. # ATCC7469) and *Bifidobacterium longum* (Cat. # ATCC15697) were applied in this study, and they were purchased from GUANGDONG HUANKAI MICROBIAL SCI&TECH Co. Ltd. *Lactobacillus rhamnosus* and *Bifidobacterium longum* were incubated in MRS medium under  $37^\circ\text{C}$  with or without oxygen.

### Cell lines

MC38 cell line (Cat. # FH0125) and MC38-OVA cell line (Cat. # FH0126) were applied in this study, and they were purchased from FuHeng Cell Center, Shanghai, China. These cell lines were cultured in RPMI 1640 Medium supplemented with 1% penicillin-streptomycin and 10% FBS under 5%  $\text{CO}_2$  at  $37^\circ\text{C}$  in a humidified incubator.

### Declaration

No human subjects were used for this study.

## METHOD DETAILS

### Preparation of probiotics formulation

Briefly, 15 mL of bacterial sub-culture were washed and resuspended in 10 mL of cold calcium phosphate solution containing 12.5 mM of  $\text{CaCl}_2$ . The mixture of DOPG and DPPC (The molar ratio of DOPG and DPPC is 17:83) is mixed with cholesterol, and dissolved in 5 mL dichloromethane at a molar ratio of 4:1. The resultant solution was dried at room temperature, using a rotary evaporator, to obtain a lipid film.<sup>21</sup> FITC-labeled coating was prepared by co-assembly with FITC-mPEG2000-DSPE (10% molar ratio to DOPG and DPPC). The obtained film was hydrated in 1 mL of bacterial solution and vortexed for 15 min and then stored at  $4^\circ\text{C}$  for further characterization.

### Characterization of probiotics formulation

A transmission electron microscope (TEM, HT7700, Hitach) was used to observe the morphology of the probiotics formulation. A drop of probiotics formulation solution was deposited on the carbon-coated copper mesh. Subsequently, the sample was observed after being completely dried in the air. The average size and zeta potential of probiotics formulation were determined by dynamic light scattering (DLS, Malvern Zetasizer nano ZS, UK) measurements. The bacteria, coated with FITC green fluorescently labeled lipid membranes (FITC-labeled lipid membranes are prepared by co-assembling mixed lipid materials with FITC-mPEG2000-DSPE), were investigated with flow cytometry analysis (FACS Calibur, USA). Additionally, the coating of RFP-expressed *Escherichia coli* was studied with laser scanning confocal microscopy (LSM 710, USA).<sup>41</sup>

### Growth curves of probiotics formulation

As described in the probiotics formulation preparation section, the bacteria were collected and washed with ice-cold PBS, and then mixed with the lipid membrane. Both uncoated *Lactobacillus rhamnosus* and probiotics formulation were diluted in MRS to an optical density 600 ( $\text{OD}_{600}$ ) value of  $\sim 0.15$ , and incubated at  $37^\circ\text{C}$  with gentle shaking. The OD values of the cultures at 600 nm were recorded every 1 h for 12 h using a microplate reader (Full-wavelength microplate reader, Switzerland).<sup>30</sup>

### Cell viability investigation of coated bacteria

The cell viability of coated bacteria was examined by CCK-8 assay. Uncoated *Lactobacillus rhamnosus* and probiotics formulation were diluted in MRS medium to an  $\text{OD}_{600}$  value of  $\sim 0.5$ . Inoculate 190  $\mu\text{L}$  of each medium in a 96-well plate and culture at  $37^\circ\text{C}$  without shaking. Add 10  $\mu\text{L}$  of CCK-8 solution to each well. Record the OD of the culture at 450 nm every 1 h with a multi-detection microplate reader (full-wavelength microplate reader, Switzerland).<sup>30</sup>

### Stability of probiotics formulation in simulated gastrointestinal tract (GI) fluids

100  $\mu$ L of probiotics formulation labeled with FITC were resuspended into 900  $\mu$ L of simulated gastric fluid (SGF), simulated intestinal fluid (SIF) or PBS, and incubated at 37°C. 100  $\mu$ L of each sample were taken at predetermined time points and examined by flow cytometry.<sup>30</sup> FITC-labeled probiotics formulation cultured in 4°C PBS was also tested to evaluate the stability of lipid coatings on the bacteria. All the solutions were sterilized by 0.22  $\mu$ m filter.

### Preparation and characterization of cancer nanovaccines reassembled from tumor tissue of MC38 colon cancer

Cancer nano vaccines, reassembled from whole tumor tissues of MC38 or MC38-OVA colon cancer, were prepared and characterized with the same as our previous published studies.<sup>32,33</sup> All components of MC38 or MC38-OVA tumor cells were loaded on cancer nano vaccines. The size of the cancer nano vaccines is around 300 nm and the zeta potential of the cancer nanovaccines is around -7mV. Cancer nanovaccines were administered the same as we previously reported.<sup>30,32,33</sup> Poly (I:C) was applied as immune adjuvants in the vaccine formulation.

Nanovaccine A (NV A) loaded with water-soluble components in tumor tissue lysates and nanovaccine B (NV B) loaded with 8M urea-solubilized non-water-soluble components in tumor tissue lysates. NV A and NV B were prepared by the double-emulsion method respectively and they were applied together as cancer vaccines. Briefly, around  $1 \times 10^6$  MC38 or MC38-OVA colon cancer cells were subcutaneous injected into the back of C57BL/6 female mice. Tumor tissue were collected when the tumor volume was around 1000 mm<sup>3</sup> and the tumor tissues were lysed as previously reported.<sup>32,33</sup> The tumor tissue lysates were centrifuged at 12000 rpm and the supernatant were collected as water-soluble components; the precipitate was non-water-soluble components and was solubilized with 8M urea. To prepare the NV A, 300  $\mu$ L of water-soluble components in endotoxin-free water (120 mg/mL, with 4 mg/mL poly(I:C) added) or non-water-soluble components in 8M urea (120 mg/mL, with 4 mg/mL poly(I:C) added) was added to 1 mL of PLGA (100 mg/mL) in dichloromethane and sonicated for 1 min. Then, the sample was added to 2.5 mL of PVA solution (20 mg/mL) and sonicated for 45 seconds. To solidify the nanoparticles (NPs), the sample was dropped into 50 mL of PVA solution (5 mg/mL) and stirred for 4 h at room temperature. The resultant NPs were collected by centrifugation for 25 min at 12,000 rpm and resuspended in 10 mL of 4% trehalose, followed by lyophilizing the NPs for 48 h. Before the administration of NV A or NV B, the nanoparticles were resuspended in 9.5 mL PBS and mixed with 0.5 mL of lysate components and 0.7 mg of poly(I:C). All the NVs were made under endotoxin-free conditions. The NVs, applied to treat mice inoculated with MC38-OVA cells, loaded with cancer cell lysates from MC38-OVA cells.

### Immunotherapy of colon cancer by NV

NVs were applied alone or together with probiotics to treat colon cancer. Tumor inoculation was performed on day 0. To treat mice, 200  $\mu$ L of NV A (containing 2 mg of PLGA) and 200  $\mu$ L of NV B (containing 2 mg of PLGA) were injected subcutaneously at different sites on day 4, day 7, day 10, day 13 and day 16. Tumour volume was recorded every 3 days beginning on day 3.

### Prevention of colon cancers by NV

NVs were applied alone or together with probiotics to prevent colon cancer. To immunize mice, 200  $\mu$ L of NV A (containing 2 mg of PLGA) and 200  $\mu$ L of NV B (containing 2 mg of PLGA) were injected subcutaneously at different sites on day -35, day -28, day -21, day -14 and day -7 ahead of tumour inoculation. Tumour inoculation was performed on day 0.

### In vivo colonization experiments

In order to verify whether lipid membrane coating can enhance bacterial colonization in the gastrointestinal tract *in vivo*, mice were gavaged with  $1 \times 10^8$  CFU of lipid membrane-coated Escherichia coli expressing biotin fluorescence (pGEN-luxCDABE). The presence and signal of probiotics were imaged at 8 h and 48 h after administration, using the Small Animal *In vivo* Imaging System (IVIS Lumina II, US) (mice gavaged with an equal volume of PBS sterile water served as a blank control). The fluorescence intensity of the gastrointestinal tract was calculated by IVIS analysis software.

### Prevention of orthotopic colon cancer

Recent research reports indicate that host-derived inflammation is an important driving force in shaping the composition of the microbial community.<sup>42,43</sup> In order to better prove that the intestinal flora is related to the occurrence and progression of colon cancer, we induced an orthotopic colon cancer model in mice and the administration of probiotic preparations were applied to prevent such orthotopic colon cancer.

Before inducing colon cancer *in situ*, mice were given probiotics and nano vaccines and the dosing schedule was as follows:

In the nano vaccines group, the nano vaccines was subcutaneously injected into the back and right thigh of the mice every seven days, for a total of five injections; the naked probiotics oral groups were orally given by gavage with 150  $\mu$ L PBS probiotics suspension containing  $1 \times 10^8$  CFU *Lactobacillus rhamnosus* and  $1 \times 10^8$  CFU *Bifidobacterium longum*, once every seven days, for a total of five times; in the probiotics formulation oral group, mice were orally given 150  $\mu$ L PBS bacterial suspension containing  $1 \times 10^8$  CFU *Lactobacillus rhamnosus* formulation and  $1 \times 10^8$  CFU *Bifidobacterium longum* formulation by gavage, once every seven days, for a total of five times; the subcutaneous injection group of naked probiotics was injected subcutaneously into mice with 50  $\mu$ L PBS bacterial suspension containing inactivated  $1 \times 10^8$  CFU *Lactobacillus rhamnosus* and  $1 \times 10^8$  CFU *Bifidobacterium longum*, and injected every seven days, for a total of five times (Put the bacterial suspension in 20 mL sterile PBS and autoclave for 20 min to prepare the bacterial antigen of the strain.); in the probiotics formulation subcutaneous injection group, 50  $\mu$ L of PBS probiotics formulation suspension containing  $1 \times 10^8$  CFU *Lactobacillus rhamnosus* inactivated antigen formulation and  $1 \times 10^8$  CFU *Bifidobacterium longum* inactivated antigen formulation was subcutaneously injected into mice, and injected every seven days, for a total of five times (the bacterial antigens of the strains were prepared by autoclaving for 20 min, and then the probiotics formulation of bacterial antigens were prepared according to the above method); the combined administration group was carried out according to the above probiotics and nano vaccines administration schedule. The probiotic was prepared by the above method.

After the administration completed, mice were i.p. injected AOM on day 0, and provided with 2% DSS through drinking water on days 5-10, 24-29, and 43-48, and normal water at other times. At the end, the mice were sacrificed on day 80 for colon tumor analysis.<sup>11,42,44</sup>

When the mice were drinking 2% DSS water, their body weight was measured every day. When the mice were supplied with normal drinking water, their body weight was measured every three days. During this period, the mice were tested for diarrhea and blood in the stool.

### Investigation of microenvironment of colon samples

In the preventative studies of orthotopic colon cancer, after 80 days, the mice were sacrificed and the colon was taken out for H&E staining, Alcian blue and periodic acid schiff (AB/PAS) staining, and immunohistochemical analysis.<sup>11,44-46</sup>

Fresh colon sections were fixed with 3.7% formalin for 24 hours, then H&E staining, AB/APS staining and immunohistochemical analysis were performed. For H&E staining, first place the fresh colon tissue in 3.7% formalin and fix it for more than 24 hours. Afterwards, the colon tissue was made into paraffin sections which were deparaffinized and washed with water, stained with hematoxylin and eosin, respectively. Following that, the sections were dehydrated and mounted for observation under a microscope. Alcian blue and periodic acid schiff (AB/PAS) staining was performed as per manufacturer's instruction to show Goblet cells. The fresh colon tissue was fixed with fixative solution for more than 24 hours and made into paraffin sections. Afterwards, they were stained with Alcian Blue, Periodic Acid, Chevron, and Hematoxylin, dehydrated and mounted, and then observed with a microscope. For IHC staining, paraffin sections were first deparaffinized and hydrated. Then the tissue sections were placed in a repair box filled with EDTA antigen retrieval buffer (pH 9.0) in a microwave oven for antigen retrieval. And they were treated with 3% hydrogen peroxide solution to block endogenous peroxidase, and block it with serum, incubate with the primary antibody at 4°C overnight, and incubate with EnVision Polymer-HRP secondary antibody (Dako) at room temperature for 30 minutes. After applying DAB chromogen (Vector), tissue sections were stained with hematoxylin, dehydrated and sealed, and observed under a microscope.<sup>11</sup>

Pathological analysis was performed for H&E staining according to published standards (Erben et al., 2014; Maxwell et al., 2015).<sup>47</sup> Tissues were scored on a 0-4 system: 0, normal; 1, mild inflammation, less than 10% loss of epithelial structures (crypts), focal enterocyte hyperplasia; 2, moderate inflammation, 10% loss of crypts- 30%, multifocal enterocyte hyperplasia, goblet cell loss; 3, obvious inflammation, crypt loss 30%-50%, diffuse enterocyte hyperplasia, goblet cells less; 4, with more than 50% crypts loss of severe inflammation, diffuse intestinal hyperplasia, mucosal ulceration. Each data point represents an individual mouse.

### **In vivo anti-cancer therapeutic evaluation**

All animal investigations were approved and monitored by the institutional ethical committee and research advisory committee of Soochow University.

The *in vivo* anti-tumor efficacy of different prepared formulations was evaluated on C57BL/6 mouse models. The colon cancer mouse model was induced by subcutaneously injected MC 38 cell line ( $2 \times 10^6$  cells/mouse) in C57BL/6 mice.

In the therapeutic studies, MC 38 cells ( $2 \times 10^6$  cells in 100  $\mu$ L of PBS) were transplanted subcutaneously into the right flank of C57BL/6 mice (6-8 weeks old). Three days later, all the mice were randomly distributed into different groups (n=8 for each group) as follows: PBS group, nanovaccines group, probiotics formulation oral group, nano vaccines + naked probiotics oral group, nano vaccines + probiotics formulation oral group, naked probiotics intratumoral injection group, probiotics formulation intratumoral injection group, nano vaccines + naked probiotics intratumoral injection group, nano vaccines + probiotics formulation intratumoral injection group.

Among them, the PBS group was injected intratumorally with 50  $\mu$ L of sterile PBS on the fourth day after tumor inoculation, once every other day, for a total of seven injections, as a blank control.

On the fourth day of tumor inoculation, the naked probiotics oral group was orally administered with 150  $\mu$ L PBS bacterial suspension containing  $1 \times 10^8$  CFU *Lactobacillus rhamnosus* and  $1 \times 10^8$  CFU *Bifidobacterium longum*; and the probiotics formulation oral group orally administered with 150  $\mu$ L PBS bacterial suspension containing  $1 \times 10^8$  CFU *Lactobacillus rhamnosus* formulations and  $1 \times 10^8$  CFU *Bifidobacterium longum* formulations by gavage. These were administered once every other day, for a total of seven times.

On the fourth day of tumor inoculation, naked probiotics intratumoral injection group was intratumor administered with 50  $\mu$ L PBS containing  $1 \times 10^8$  CFU of *Lactobacillus rhamnosus* and  $1 \times 10^8$  CFU of *Bifidobacterium longum*; and probiotics formulation intratumoral injection group was intratumor administered with 50  $\mu$ L PBS containing  $1 \times 10^8$  CFU of *Lactobacillus rhamnosus* formulation and  $1 \times 10^8$  CFU of *Bifidobacterium longum* formulation. These were administered every other day, for a total of seven times.

The nano vaccines group was subcutaneously administered from the fourth day of tumor inoculation, and one injection was subcutaneously injected to the back and thigh of the mouse every three days, for a total of five injections. The preparation method of nano vaccines and characterization of nano vaccines were the same as our previous studies.<sup>30,32,33</sup>

The probiotics combined with nano vaccines group were co-administered according to the above dosing schedule.

The weight of mice and the tumor size were monitored from day 0, and they were recorded every 3 days. At the same time, the survival rate was also monitored. Use the following formula to calculate the tumor volume. Tumor volume was calculated as follow: Tumor volume =  $0.52 \times (\text{length of the tumor}) \times (\text{width of the tumor})^2$ . When the tumor volume in mice exceeded 2000  $\text{mm}^3$ , the mouse was recognized as dead and sacrificed, and the splenocytes were collected to analyze the amount of tumor antigen -specific T cells.

### **Analysis of tumor antigen-specific T cells in splenocytes of treated mice**

The analysis of tumor antigen-specific T cells in splenocytes of treated mice was analyzed with flow cytometry. The studies are conducted as follows: C57BL/6 mice were inoculated with MC 38 cell line ( $2 \times 10^6$  cells/mouse) or MC38-OVA cell line ( $2 \times 10^6$  cells/mouse) on day 0. Nano vaccine and/or bacteria formulation (or supernatant of bacterial culture media in  $1 \times 10^8$  CFU bacteria) were administered the same as in

therapeutic studies. Mice were sacrificed on day 15 after tumor inoculation, followed by collecting mouse splenocytes. The splenocytes were con-incubated with whole tumor antigens in tumor lysates or OVA peptide (OVA<sub>257-264</sub> or OVA<sub>323-339</sub>) for 16 h in a cell incubator at 37°C, and 2 mL of BFA solution was added to each well. And then, splenocytes were harvested for 4 h, followed by samples incubating with Fc blocker. And then, the cells were surface stained with anti-mouse antibodies against CD3, CD4, and CD8. Following fixation, membranes were ruptured, and intracellular antibody staining was performed with IFN- $\gamma$ <sup>+</sup>. And then, the flow cytometric analysis was applied to study the secretion of IFN- $\gamma$  by CD4<sup>+</sup> T cells and CD8<sup>+</sup> T cells, upon stimulating with antigens. The flow software analysis was used to show the percentage of CD8<sup>+</sup> IFN- $\gamma$ <sup>+</sup> cells in the CD8<sup>+</sup> T cell population or the percentage of CD4<sup>+</sup> IFN- $\gamma$ <sup>+</sup> cells in the CD4<sup>+</sup> T cell population.

### Analysis of the tumor infiltrating lymphocyte populations

C57BL/6 mice were inoculated with MC 38 cell line ( $2 \times 10^6$  cells/mouse) on day 0. Nano vaccine and/or formulation (or supernatant of bacterial culture media in  $1 \times 10^8$  CFU bacteria) were administered the same as in therapeutic studies. Mice were sacrificed on day 15 after tumor inoculation, followed by collecting mouse tumor tissues for flow cytometric analysis. Single-cell suspensions were prepared using collagenase/hyaluronidase and DNase. Before surface staining, the samples were incubated with Fc Block for 5 min, followed by surface staining with anti-mouse antibodies against CD45, CD3, CD8, CD25, CD49b, CD11c, F4/80 and CD4. Cells were then fixed, permeabilized, and stained for intracellular FOXP3 and IFN- $\gamma$ . Flow cytometric analysis was performed using a FACS AriaTMIII and analyzed using FlowJo 10 software. Differences were compared by a t-test.

### Prevention of colon cancer in subcutaneous cancer mouse model

The preventive efficacy of various formulation was first studied in subcutaneous cancer mouse model. The probiotic formulations were preventatively administered (oral or subcutaneous injection) before tumor inoculation. The dosing schedule of each group of mice is as above.

After the preventative treatment, MC 38 cells ( $2 \times 10^6$  cells in 100  $\mu$ L of PBS) were injected subcutaneously into the right flank of C57BL/6 mice (6-8 weeks old).<sup>48-50</sup>

The body weight of mice was measured once a week during dosing. After tumor inoculation, the survival rate, body weight and the tumor volume were monitored every three days. The tumor volume was calculated as follow: Tumor volume =  $0.52 \times (\text{length of the tumor}) \times (\text{width of the tumor})^2$ . Once the tumor volume in mice exceeded 2000 mm<sup>3</sup>, the mouse was recognized as dead and sacrificed. Then, the main organs, such as kidney, lung, spleen, liver and heart, were collected, washed with PBS, and fixed in 10% neutral buffered formalin solution, until paraffin embedding. Subsequently, the tissue block is cut into 4-5  $\mu$ m diameter using a standard rotary microtome and staining procedure. Sections were stained with hematoxylin and eosin (H & E), and observed under microscope.

### QUANTIFICATION AND STATISTICAL ANALYSIS

Statistical differences in mean tumor growth curves were determined by two-way ANOVA using time and volume variables. Survival differences among groups were determined by the Kaplan-Meier method, and overall P-values were calculated by the log-rank test. All of the statistical details of experiments can be found in the figure legends and [method details](#). Statistical differences in flow cytometry analyses were compared by t-test, one-way ANOVA. All statistical analyses were done using GraphPad Prism 8.0.2.